Adjuvanting Coxevac® with QuilA® skews Coxiella burnetii-induced inflammatory responses towards a sustained Th1-CD8+-mediated activation and increases protection in an experimental goat model

Sara Tomaiuolo
Sciensano
Wiebke Jansen
Sciensano
Susana Soares Martins
Sciensano
Bert Devriendt
Ghent University
Eric Cox
Ghent University https://orcid.org/0000-0003-4281-2990
Marcella Mori (marcella.mori@sciensano.be)
Sciensano

Article

Keywords: C. burnetii, QuilA, goat model, CD8+IFN, proinflammatory response, Principal Component Analysis

Posted Date: August 19th, 2022

DOI: https://doi.org/10.21203/rs.3.rs-1897579/v1

Adjuvanting Coxevac® with QuilA® skews *Coxiella burnetii*-induced inflammatory responses towards a sustained Th1-CD8+-mediated activation and increases protection in an experimental goat model

Sara Tomaiuolo[1,2,3], Wiebke Jansen[1,2], Susana Soares Martins[1], Bert Devriendt[3], Eric Cox[3], Marcella Mori[1,2*]

[1] Bacterial zoonoses unit, Veterinary Bacteriology, Infectious diseases in animals Scientific directorate, Sciensano, Brussels, Belgium

[2] National Reference Centre for *Coxiella burnetii* and *Bartonella,* Belgium

[3] Laboratory of Immunology, Department of Translational Physiology, Infectiology and Public Health, Faculty of Veterinary Medicine, Ghent University, Merelbeke, Belgium

ABSTRACT

Coxevac® is the EMA-approved veterinary vaccine for the protection of cattle and goats against Q Fever, a zoonotic bacterial disease due to *Coxiella burnetii*. Since Coxevac® reduces bacterial shedding and clinical symptoms but does not prevent infection, novel, ready-to-use vaccine formulations are needed to increase its immunogenicity. Here, a goat vaccination-challenge model was used to evaluate the impact of the commercially available saponin-based QuilA® adjuvant on Coxevac® immunity. Upon challenge, the QuilA®-Coxevac® group showed a stronger immune response reflected in a higher magnitude of total IgG and an increase in circulating and splenic CD8+ T-cells compared to the Coxevac® and challenged-control groups. The QuilA®-Coxevac® group was characterized by a targeted Th1-type response (*IFNɣ, IP10*) associated with increased transcripts of CD8+ and NK cells in spleens and γδ T cells in bronchial lymph nodes. Coxevac® vaccinated animals presented an intermediate expression of Th1-related genes, whilst the challenged-control group showed an immune response characterized by pro-inflammatory (*IL1β, TNFα, IL12*), Th2 (*IL4* and *IL13*), Th17 (*IL17A*) and other immunoregulatory cytokines (*IL6, IL10*). An intriguing role was observed for γδ T cells, which were of TBX21- and SOX4-types in the QuilA®-Coxevac® and challenged control group, respectively.
Overall, the addition of QuilA® resulted in a sustained Th1-type activation associated with increased vaccine protection. QuilA® could be proposed as one readily-applied solution to improve Coxevac® efficacy against *C. burnetii* infection in field settings.

Keywords: *C. burnetii*, QuilA, goat model, CD8+IFNɣ, proinflammatory response, Principal Component Analysis

INTRODUCTION

Q fever is a zoonotic bacterial infection leading to significant public health and economic issues worldwide. The causative agent, C*oxiella burnetii,* is a highly infectious intracellular Gram-negative bacterium, which is extremely resistant in the environment[1]. In ruminants, *C. burnetii* infection causes abortion, stillbirth and infertility, but distinct clinical outcomes are observed between ruminant species: abortion storms in goats and sheep, and sporadic abortion cases in cattle[2,3]. The parturition or immediate postpartum periods are those at the highest risk in terms of bacterial shedding, however, the excretion might occur also beyond these periods by clinically affected or asymptomatic animals[4,5].

Knowledge about the pathogenesis of *C. burnetii* and the associated immune responses in domestic ruminants is scarce. In pregnant goats, bacterial replication starts in the trophoblasts of the allantochorion[6–8]. Bacterial DNA can be detected in the placenta 4 weeks post-infection (wpi), suggesting that *C. burnetii* needs time to multiply until reaching detectable levels[8]. Massive bacterial multiplication occurs however in the last weeks of gestation, before abortion[7]. From 6 wpi, *C. burnetii* DNA can also be present in other organs than the placenta[8]. Whether the function of these infected organs is affected by the presence of *C. burnetii* is yet unknown.
Infection of goats with *C. burnetii* induces considerable antibody responses, indicating that humoral immunity contributes to the defense mechanisms against Q fever. A similar magnitude of antibody responses has been observed in pregnant and non-pregnant goats[9,10]. In both, IgM and IgG antibodies against *C. burnetii* phase 2 (avirulent) antigens appear from 3 wpi onwards. In non-pregnant goats, phase 1 (virulent) IgM and IgG titers increase after 3 and 4 wpi, respectively. This anti-phase 1 antibody response is delayed in infected pregnant goats.
Although cell-mediated immune responses are important for protection against infection with intracellular pathogens, both the nature of the induced cell-mediated immune responses and their role in protecting goats from infection with *C. burnetii* remain poorly described. Roest et al.[9] showed that cytokine mRNA levels in peripheral blood of pregnant goats increased before (*IL10*) or after (*TNFα, IL1β)* parturition. This coincided with an up-regulation of the total IFNγ production in peripheral blood mononuclear cells (PBMCs) at one-week post parturition[9]. Ammerdorffer et al.[11] also observed increased *IFNγ* and *TNFα* transcript levels in antigen-stimulated PBMCs from infected pregnant goats. Thus, although some studies reported changes in cytokine production by PBMCs in pregnant goats, the identity of the involved cells remains unknown. In addition, no information is available regarding non-pregnant goats.

A deeper understanding of the pathogenesis of *C. burnetii* and the immune responses raised upon infection of domestic ruminants may contribute to the redefinement and the improvement of ruminant vaccines, deployed as a preventive measure to limit Q fever in animals and halt transmission to humans. In Europe, the Coxevac® non-adjuvanted whole-cell formalin-inactivated phase 1 vaccine (Ceva Santé Animale, Libourne, France) is used to protect cattle and goats against Q fever[12]. Although several studies demonstrated its efficacy in reducing clinical signs (abortions) and bacterial shedding[13–16], this vaccine does not prevent infection[13,15] nor clears the infection in infected animals[17,18]. In addition, field data indicated that antibody levels decrease after 9 months below protective levels, hampering targeted annual vaccination programs on herd level[19]. If the critical level of protective immunity is not maintained long enough at the individual or herd level, recrudescence will likely take place[19,20]. In this case, consistent control of *C. burnetii* infection in ruminants is only reached through the use of costly and multiannual compliant vaccination protocols[14,19].

Many vaccines require the addition of adjuvants to induce an appropriate immune response for protection upon challenge. Adjuvants are able to increase the magnitude of the vaccine induced-immune responses, and, importantly, to tailor immune responses to each specific pathogen. Indeed, certain adjuvants can drive specific immune responses (i.e $CD4^+$ vs $CD8^+$ T cells, Th1 vs Th2 response,

distinct antibody isotypes), encourage immune memory responses or activate a quicker initial response[21]. QuilA®, a saponin adjuvant extracted from *Quillaria saponaria*, is widely used in veterinary vaccines due to its capacity to stimulate both $CD4^+$ helper and $CD8^+$ cytotoxic cells as well as to induce long-lasting antibody responses[22–27]. It is an EMA-approved veterinary medicinal product and therefore immediately applicable in field settings. Considering both the non-adjuvanted nature of Coxevac® and the QuilA®-driven induction of T cell immunity, we selected this adjuvant as a candidate for improving the efficacy and immunogenicity of Coxevac®.

In this study, we characterized the immune response induced by Coxevac® vaccination and evaluated the influence of QuilA® on vaccine immunogenicity and efficacy in goats. In order to mimic natural infections, goats were challenged for the first time with an aerosolized axenic culture of *C. burnetii,* isolated from an infected goat in 2010. Considering the intracellular nature of the bacterium, obtaining an axenic culture from field samples is extremely rare and challenging. Our data demonstrated that Coxevac® did not generate an immune response able to confer substantial protection upon challenge. However, the addition of the QuilA® adjuvant enhanced the humoral response and induced a sustained Th1-type cellular response resulting in increased vaccine efficacy.

RESULTS

1. *In vitro* and *in vivo* quality controls of the bacterial inoculum

The CbBEC2 strain was previously isolated in axenic medium at the National Reference Centre. As the infective capacity of *C. burnetii* strains is determined by the expression of a phI LPS[28], we verified the presence of a full-length LPS in this strain. The existence of genes involved in the synthesis of a phI LPS was investigated by WGS. The alignment of the CbBEC2 assembly and the NM phI DNA sequence (encoding for the operon involved in the biosynthesis of the complete LPS) resulted in 99.92 % similarity, indicating an operon genetic integrity in the CbBEC2 strain. The complete LPS sequence was localized in contig 11 as illustrated in Figure 2A. To further examine the phase properties of the LPS, CbBEC2 at passage 6 (P6) was cultivated for 14 days in ACCM-2 and LPS was isolated and profiled on a silver-stained gel (Figure 2B). The phI pattern of CbBEC2 LPS was unique and differed from that of NM phI LPS (bands above 10 kDa). As LPS was isolated from the CbBEC2 strain at P6, we observed co-appearance of intermediate (around 10 kDa) and minor presence of phase II (far below 10 kDa) LPS forms. These LPS features could be attributed to the serial passages[29] or the intrinsic nature of the strain[30]. To verify that the infectious potential of the CbBEC2 axenic cultures (P6) was retained after passages, we compared the proliferative capacity of CbBEC2 from freshly collected splenic harvest at P2 (estimated m.o.i. of $5x10^3$ G.E.) to that from the axenic culture at P6 (estimated m.o.i. of $4*10^3$ G.E.) in a mouse model. The axenic culture at P6 triggered significantly higher bacterial loads than the P2 in the spleen (Figure 2C, mean w1-w4 of $7.7x10^5$ G.E./g vs $5.3x10^4$ G.E./g) and equivalent loads in the liver and the lungs (data not shown). Also, the axenic strain triggered significantly higher organ weights in the spleen and liver and significantly higher IgM and IgG levels (Figure S1). Overall, these results validated the infectivity, the genetic features and the quality of the inoculum prepared from CbBEC2 cultures P6, which will be used for a challenge infection in the subsequent experiment.

2. Vaccination-challenge experiment in goats

Effective action of Coxevac® is usually achieved following compliant multiannual vaccination protocols, but filed data indicated that protective antibody levels are not maintained long enough to establish standardized yearly vaccination programs[19]. Given that Coxevac® does not contain an adjuvant and the need to increase its efficacy, we designed an improved formulation of Coxevac® by including the ready-to-use QuilA® adjuvant in the emulsion. This new formulation was assessed in a vaccination-challenge

experiment using Saanen goats and inocula prepared from axenic cultures of the CbBEC2 strain (P6) (Figure 1).

2.1 QuilA®-Coxevac® prime vaccination induces a transient increase of the rectal temperature

None of the control and the Coxevac® goats experienced severe hyperthermia (>40°C), as indicated by the rectal temperature, at any time point after prime vaccination or boost (Figure 3A). One day after prime vaccination, all animals from the QuilA®-Coxevac® group presented a rise in the rectal temperature (average of 39.9°C ± 0.5), with three goats experiencing severe hyperthermia on days 1 to 3 (Figure 3B). After challenge, no major changes were observed in the groups, although a slight increase of the average temperature was observed in the control few days post-challenge. One goat (V2) of the Coxevac® group experienced severe hyperthermia from day 32 post-challenge towards the end of the experiment (Figure 3B) and presented clinical signs attributable to mastitis (the left mammary gland was hard, swollen, reddish and sensitive to touch).

2.2 QuilA®-Coxevac® vaccination induced a robust and sustained anti-*C. burnetii* IgG response and an increased protection efficacy against Q Fever

After vaccination, IgG antibodies against *C. burnetii* were significantly more protracted in the QuilA®-Coxevac® than in the Coxevac® group (4 to 12 wpv vs 4 to 9 wpv) as opposed to the control goats (Figure 4A). The first goat that reached levels above the threshold defined by the ELISA assay was detected at 2 wpv in goats vaccinated with QuilA®-Coxevac®, whilst only at 4 wpv in the Coxevac® goats (Figure 4B). All goats from the Coxevac® and QuilA-Coxevac® groups exceeded the threshold after 5 and 6 wpv, respectively.

Upon challenge, the first goat of the control group that crossed the threshold level was detected at 16.5 wpv (3.5 weeks post-challenge, wpc) and an increase in the total IgG production was reached at 18 wpv (5 wpc) (Figure 4B). Throughout the experiment, two control goats remained below the threshold defined by the ELISA assay. In the vaccinated groups, IgG levels rose again at 17.5 and 18 wpv in the Coxevac® and QuilA®-Coxevac® goats, respectively. After the challenge, the magnitude of the induced IgG antibodies was significantly higher in the QuilA®-Coxevac® group compared to control and Coxevac® animals (73% S/P vs 18% S/P and 43% S/P, respectively), while the control and Coxevac® group did not differ significantly in IgG levels (Figure 4A).

As humoral immunity plays a role in the protection against Q Fever[31–33], we assessed whether vaccination with Coxevac® and QuilA®-Coxevac® was associated with increased protection. The presence of *C. burnetii* was investigated in several organs (n = 28) and blood after sacrifice (Table 1, S2 and S3). The detection limit of the PCR assay was reached considering that results on DNA extracted from tissues were negative. Thus, splenocytes and bronchial lymph node cells were injected in embryonated eggs for bacterial amplification. An animal was considered positive if at least one of the two results was positive. *C. burnetii* was detected in 100% of the control and Coxevac® goats and 66.6% of QuilA®-Coxevac® goats (Table 1). Also, bacteremia was evaluated in all challenged goats at selected time points post-infection by PCR (Table S3). In vaccinated goats, bacteremia was principally detected 1-day post-challenge. Taken together, these results confirmed that all goats were successfully infected with *C. burnetii* CbBEC2 strain and that QuilA® increased the Coxevac®-induced IgG response and protection.

2.3 Differential IFNγ secretion profiles upon antigen-specific stimulation of PBMCs

To further explore cell-mediated immunity upon vaccination and challenge, we assessed the antigen-specific IFNγ response. PBMCs were *ex vivo* stimulated with *C. burnetii* antigens and the IFNγ production was measured at different time points. Upon vaccination, the IFNγ secretion profile in the Coxevac® group was detected as a unimodal response with a peak at 5 wpv (after the boost vaccine dose, 61% S/P). In contrast, the IFNγ kinetics of the QuilA®-Coxevac® group resulted in a bimodal response with the first peak of IFNγ production after the prime (2 wpv, 45% S/P) and the second peak

after the booster (5 wpv, 25% S/P) vaccination (Figure 4C). Upon challenge, completely different IFNγ patterns were observed for the three groups. In the control group, moderate levels of IFNγ production were detected immediately after the challenge (13.5 wpv), followed by a sudden increase at 17-17.5 wpv (4-4.5 wpc) and maintained until the end of the experiment. The IFNγ response of the Coxevac® group remained moderated and stable until the end of the experiment. In contrast, a bimodal trend characterized again the response of the QuilA®-Coxevac® group with the highest peak detected promptly after the challenge (13.5-14 wpv) and a second peak at 17.5-18 wpv. The mixed-effects model corroborated statistically significant differences between the three patterns post-challenge. This is illustrated by the interaction between time and group variables of control and Coxevac® ($F(13, 102) = 5.02$; $p < 0.0001$), control and QuilA-Coxevac® ($F(13, 102) = 4.5$; $p < 0.0001$), Coxevac® and QuilA®-Coxevac® ($F(13,129) = 1.96$; $p < 0.02$) groups.

2.4 The two Coxevac® formulations activate different immune cell subsets upon challenge

Considering the differential IFNγ recall response observed in the three groups, we next assessed whether these differences could be attributed to distinctive activation of lymphocyte subpopulations. Therefore, we investigated the kinetics of T ($CD4^+$ and $CD8^+$) and B ($CD21^+$) cells in PBMCs upon vaccination and challenge (Figure 5A). The frequency of $CD4^+$ and $CD21^+$ cells did not change between groups after vaccination nor challenge (Figure 5B). Likewise, vaccination did not influence the percentage of $CD8^+$ cells detected before challenge, however, vaccinated groups showed significantly different patterns as compared to the control group after challenge. The results were validated with the mixed-effects model analysis that revealed a significant interaction between time and group variables of the control and Coxevac® ($F(8, 64) = 2.48$; $p < 0.02$) and control and QuilA®-Coxevac® ($F(8, 64) = 2.68$; $p < 0.01$) groups. At 19 wpv, the $CD8^+$ frequency in PBMCs was higher in animals vaccinated with QuilA®-Coxevac® compared to the Coxevac® group (Figure 5B). This $CD8^+$ population was also strongly present in splenocytes of the QuilA®-Coxevac® group at sacrifice (28.0% in QuilA-Coxevac® vs 15.9% in control and 18.3% in Coxevac®) (Figure 6A). Interestingly, the increased frequency of $CD8^+$ cells in spleens was associated with an increased frequency of a granulocytic population (3.4% in QuilA®-Coxevac® vs 1.1% in control and 1.8% in Coxevac®) (Figure 6B). The frequency of the other sub-populations was comparable between groups in all investigated organs (Figure 6A, Figure S2).
For the $CD4^-CD8^-$ cell population in PBMCs, the mixed-effects model did not identify different patterns between groups ($F(16, 104) = 0.7$; $p = 0.7$), but revealed significant differences in the average $CD4^-CD8^-$ frequency between groups post-challenge ($F(2, 13) = 4.803$; $p < 0.02$). At several time points (13, 13.5, 15, 16, 18, 19 wpv), significant pairwise differences between the Coxevac® and QuilA®-Coxevac® group were present. Additionally, at 19 wpv, the $CD4^-CD8^-$ frequency in the Coxevac® group was also significantly higher compared to control goats (Figure 5B). To provide a deeper characterization of this $CD4^-CD8^-$ cell subpopulation, we looked at γδ T cells and $WC1^+$ γδ T cells at 13.5 and 19 wpv. However, no significant differences in the relative percentage were observed between groups in these cell populations (Figure S3).

2.5 Distinctive transcriptional patterns are induced in spleens and bronchial lymph nodes of vaccinated and control animals upon challenge

We next sought to further investigate the immune responses activated by the different conditions. As such, we studied the expression profiles of 23 selected genes (comprising cytokines, CDs, receptors and transcription factors) in splenocytes and bronchial lymph node cells upon infection (Figure 7 and 8). Vaccination with QuilA®-Coxevac® skewed the transcriptional gene expression induced by infection towards an increased expression of *CD8, NRC1* and the Th1 cytokine *IFNɣ* in spleen, corroborating the previous results of cell phenotyping and IFNɣ production. In this organ, the expression of *IL1β, IL17a, CD11b* and *TRGC2* was instead more expressed upon challenge in the Control group than in the other two groups (Figure 7A). Gene expression in the respiratory lymph nodes highlighted the differences

among groups. Here, *IL12p40, IL6* and *CD11b* were more expressed upon challenge in the Control group than in vaccinated groups. *TLR6* was also significantly more expressed in the Coxevac® compared to the QuilA®-Coxevac® group (Figure 8A).
To highlight specific transcriptional patterns, the relative gene expression was further used for high-level comparative analyses. In both splenocytes and bronchial lymph node cells, three different clusters were identified (Figures 7B and 8B). The first cluster regrouped genes highly and intermediately expressed in the QuilA®-Coxevac® and Coxevac® groups, respectively. These genes included *IFNɣ, CD8, NRC1* and *IP10* in splenocytes and *TBX21*, *TRGC2* and *IP10* in bronchial lymph nodes. The second cluster represented genes more expressed in challenged-control goats than the challenged-vaccinated groups. In splenocytes, it regrouped pro-inflammatory cytokines (*IL1ß, TNFα*), Th2 cytokines (*IL4* and *IL13*), *IL17a* and *IL10*, as well as *CD11b* and *TRGC2* cellular markers and the *SOX4* transcription factor. In bronchial lymph nodes, it consisted again of *IL4, IL13, IL17a* and *CD11b*, but included *IL6* and *IL12* as well. The third cluster comprised genes that were homogeneously expressed in all groups or for which a specific pattern was unclear.

2.6 Specific immune responses distinguish Coxevac®, QuilA®-Coxevac® and control goats following *C. burnetii* challenge

In an attempt to reduce noise and extract representative information from the entire dataset to highlight immune patterns activated distinctly by vaccinated and control goats upon *C. burnetii* infection, we used the pattern recognition approach through the principal component analysis (PCA). When we used the complete dataset (n = 68), which includes data from serology (13.5, 17.5 and 19 wpv), IFNɣ secretion upon antigen-specific stimulated PBMCs (13.5, 17.5 and 19 wpv), organ and blood (19 wpv) phenotyping and gene expression profiles, we observed that vaccinated animals from the two groups, Coxevac® and QuilA®-Coxevac®, were separated in two clusters (Figure 9A). In these groups, even if crossing areas were present, the intra-group variance (σ^2) was reduced compared to the control group ($\sigma^2_{Coxevac} = 0.71$, $\sigma^2_{QuilA\text{-}Coxevac} = 0.99$ vs $\sigma^2_{Control} = 1.35$). Conversely, within the control group, the higher intra-group variance highlighted the different responses among animals in this group, in particular for the C1 goat, who was the least responsive upon challenge. Overall, when considering a high level of complexity of variables, the three groups were quite close in both 2D and 3D plots (Figure 9A). In contrast, selecting specific variables (n = 22) to reach distinctive clusters among conditions, characteristic features that can accurately describe each group were identified (Figure 9B). The control group was distinguished by cytokines (i.e. *IL1ß, IL12, IL6, IL17a*), CD11b cells in the secondary lymphoid organs, γδ T cells in spleen and IFNɣ secretion upon antigen-specific stimulation of PBMCs. The Coxevac® group had a distinctive feature, the $CD4^-CD8^-$ lymphocyte population present in both systemic and secondary lymphoid organs. Finally, the QuilA®-Coxevac® group was distinguished by its increased IgG response, the higher frequency of $CD8^+$ T cells in blood and secondary lymphoid organs, and by a greater expression of *CD8*, *NRC1* and *IFNɣ* in the spleen.

DISCUSSION

In the present study, we aimed to characterize the immune responses elicited by Coxevac® vaccination upon challenge infection of goats with *C. burnetii* and to evaluate its efficacy when complemented with an adjuvant. As the T cell-mediated immunity is critical for protection against Q Fever, the QuilA® adjuvant, an EMA-approved veterinary medicinal product, was selected as a candidate for improving Coxevac® efficacy. Adjuvanting vaccines with QuilA® triggers more robust humoral and cellular immune responses against a wide range of pathogens than the non-adjuvanted forms[34–37]. For the first time, an axenic culture of *C. burnetii*, isolated from a field sample, was used to produce the challenge inoculum. Before intranasal inoculation of goats with the CbBEC2 strain, we assessed the presence of a full-length LPS, crucial for virulence of *C. burnetii*. In the mouse infection model, the infectious potential of the axenic inoculum was higher than the CbBEC2 inoculum derived from freshly collected

splenic harvest, demonstrating the suitability of axenic culture for the preparation of the challenge dose.

In our experimental study, the humoral immunity was evaluated after vaccination and challenge in a caprine model by determining *C. burnetii*-specific IgG levels. Both vaccination regimes, Coxevac® and QuilA®-adjuvanted Coxevac®, induced antigen-specific IgG, whilst only the adjuvanted form was able to stimulate a protracted antibody response after vaccination. Upon challenge, the QuilA®-Coxevac® group mounted a stronger humoral response compared to both the challenged-control and the Coxevac® group. These results indicated that QuilA® enhanced circulating IgG antibodies against *C. burnetii* in goats vaccinated with Coxevac®. The role of the humoral response for protection against *C. burnetii* is still undetermined in goats. In small animal experimental models, adoptive transfer of immune sera from vaccinated mice to SCID mice prevents significant weight loss, but exclusively adoptive T cell transfer can prevent splenomegaly and reduce splenic bacteria burden upon challenge[33]. Therefore, in the murine model, the humoral response is critical for the prevention of clinical disease, but not for infection control. Surprisingly, the antibody response generated by challenged control and Coxevac® goats was comparable. It suggests that the reduction of clinical symptoms, such as abortions and bacterial shedding, observed in goats after vaccination with Coxevac® does not rely exclusively on antibody production[13–16]. At sacrifice, live *C. burnetii* were detected in spleens and/or bronchial lymph nodes of all challenged control and Coxevac® goats, confirming that vaccination with Coxevac® is insufficient to prevent the infection[13,15]. However, *C. burnetii* DNA was under the detection limit of the PCR assay requiring bacterial sample pre-amplification in embryonated eggs. Globally, the infection was associated with a low bacterial burden in all groups. Reasons for the low infection rate could be explained by the absence of breeding in our animals[10] or the different kinetic of infection of our strain in relation to a previous study[8]. Interestingly, vaccination with QuilA®-adjuvanted Coxevac® induced a moderate but increased protection efficacy. The robust IgG response initiated by this group may have contributed to mounting an immune response favoring *C. burnetii* clearance.

However, specific antibodies are often not sufficient to induce significant protection in infections caused by intracellular pathogens. In such cases, including *C. burnetii* infection, cell-mediated immunity is essential for eliciting protective responses. In mice, despite both T and B cells being required for protective immunity, only T cell-mediated immunity is critical for protection against Q Fever[33,38]. Additional studies showed the importance of IFNγ in the host defense against *C. burnetii* for controlling bacterial replication and elimination[13,39–43]. To assess cellular *C. burnetii*-specific responses, PBMCs were *ex-vivo* stimulated in an antigen-specific manner and IFNγ was measured upon vaccination and challenge of goats. In the Coxevac® group, a peak of IFNγ production was reached only one week after the booster dose, at 5 wpv. In contrast, in the QuilA®-Coxevac® group, a first peak was detected two weeks after the prime vaccination and a second peak one week after the boost (5 wpv). These results suggest that (1) the reaction time for IFNγ production was reduced to one week between the prime and the booster dose in the QuilA®-Coxevac® group and (2) the antigen-specific IFNγ response was accelerated by QuilA®-Coxevac® vaccination compared to Coxevac® only. Thus, we hypothesize that QuilA® favored the process of antigen uptake and presentation to promote enhanced immunomodulation which accelerated IFNγ responses. The mechanism of action of QuilA® remains poorly understood, but the current model entails that the lipophilic moiety of Quillaja saponins promotes direct delivery of exogenous antigens to the intracellular cell compartment of antigen-presenting cells (APCs). The antigen, processed within the endocytic pathway, leads to MHCI class presentation with consequent $CD8^+$ cells stimulation[44]. Other saponin-derived adjuvants, such ISCOMs or Q21, can improve antigen uptake as well as T cell and antibody responses[45–48].
Upon challenge, a bimodal pattern characterized again the IFNγ response generated by antigen-stimulated PBMCs of the QuilA®-Coxevac® group, with the highest peak detected immediately after challenge (13.5 wpv) and a second peak at 17.5 and 18 wpv. Considering that goats were exposed to

C. burnetii antigens during vaccination, the prompt response of this group could be attributed to a direct consequence of this exposure. By contrast, the minor response of the Coxevac® group upon challenge suggests that Coxevac® vaccination alone is unable to induce such a response. One hypothesis is that Coxevac® vaccination could activate different pathways or lymphocyte subsets, leading to an IFNγ-independent response, as supported by the higher frequency of $CD4^-CD8^-$ cells detected in PBMCs of this group after challenge. The $CD4^-CD8^-$ population is involved in the control of intracellular bacteria, such as *Mycobacterium tuberculosis* or *Francisella tularensis* Live Vaccine Strain (LVS), and may contribute to protection [49]. Further research is needed to identify this population and its role in inducing protective immunity.

In challenged control goats, an antigen-specific IFNγ response was detected quickly upon challenge until the end of the experiment, meaning that *C. burnetii* infection induced a long-term production of IFNγ by PBMCs in a recall assay. This response was characterized by two phases: an initial moderate production promptly after challenge (13.5 wpv) followed by a sudden increase at 17-17.5 wpv (4-4.5 wpc). This second wave corresponded to the second IFNγ peak detected in the QuilA®-Coxevac® group. Four weeks could be the time needed to mount the adaptive response against *C. burnetii*, or relates to the kinetic of bacterial multiplication *in vivo*. Indeed, in pregnant goats, *C. burnetii* DNA has been detected in the placenta of infected animals only from 4 wpi onwards[8]. The strong IFNγ response induced in the challenged control goats by stimulated PBMCs may reflect a pronounced systemic infection, probably due to a lack of control in secondary lymphoid organs. In this group, the transcriptional pattern of spleens and respiratory lymph nodes showed indeed an immune response characterized by cytokines, such as pro-inflammatory (*IL1β, TNFα, IL12*), Th2 (*IL4 and IL13*), Th17 (*IL17a*) and immunoregulatory cytokines (*IL6, IL10*). Increased levels of IL10, TNFα and IL1β were previously described in peripheral blood of infected pregnant goats before or after parturition[9]. IL1β, IL6 and TNFα production were higher in natural infected individuals compared to vaccinated ones[50]. Also, increased levels of inflammatory cytokines (i.e. TNF, IL6, IL12, IL10, IL1b) characterize patients with both acute and chronic Q Fever[51–54]. Cytokine overproduction was detected in patients with high risk of developing the chronic form of Q Fever: the chronic course is related to intense inflammation, determined by the upregulation of TNF, IL1b, IL6 and excessive IL10 expression[51–53]. It was shown that IL10 supports the intracellular replication of *C. burnetii* by inhibiting the microbicidal capacity of monocytes and macrophages[55–57]. Ghigo et al.[58] showed that also IL4 promotes *C. burnetii* replication in human monocytes. Indeed, IL10 shares with the Th2 cytokines, IL13 and IL4, the ability to redirect the polarization status of macrophages toward an M2 program, promoting anti-inflammatory responses and wound healing[59]. Benoit et al.[60] proposed a model of monocyte and macrophage polarization following *C. burnetii* infection: monocytes activating M1-associated molecules are able to control bacterial replication; macrophages inducing an atypical M2 program in response to *C. burnetii* permit a moderate replication of the bacteria, as observed in acute Q Fever; monocytes and macrophages triggering a complete M2 polarization are permissive for bacterial replication, similar to chronic Q Fever. New candidate vaccines inducing a Th2-biased response did not confer a similar protection as Q-Vax, the licensed human vaccine against Q Fever[61]. Q-Vax induces a Th1-dominant response that is critical for effective protection against Q Fever[33,62]. Overall, IL10 and Th2 cytokines seem to interfere negatively with the control of Q Fever. Thus, the overexpression of these cytokines in secondary lymphoid organs of challenged control goats may have hampered the establishment of an effective immune response capable to confine *C. burnetii* to organs and to control the infection.

The immune response initiated by QuilA®-Coxevac® goats was more targeted and limited at the local level. An increased frequency of a granulocytic population was detected in spleens of the QuilA®-Coxevac® group. In the mouse model, eosinophils and neutrophils are involved in vaccine protection against Q Fever[63,64]. Neutrophil accumulation was detected within tissues of mice infected with the virulent NM phI strain compared to the avirulent NM phII strain[65]. These findings suggest a role for granulocytes in protective immune responses against *C. burnetii*, which we showed might be true also

in the goat model. Interestingly, the expression level of *CD11b*, used as a marker for several cell types such as granulocytes, macrophages, NK cells, B lymphocytes and dendritic cells, was significantly increased in challenged control goats compared to the vaccinated-challenged groups. The specificity of this marker should be better investigated in goats, together with its role during *C. burnetii* infection. The QuilA®-Coxevac® group was characterized by an increase in the $CD8^+$ T cell frequency in spleens and PBMCs (at 19 wpv) compared to the other groups. The transcriptional pattern of this group included genes, such as *CD8*, *NRC1* (NK cell receptor), *IP10* and *IFNɣ*, which were more expressed in the QuilA®-Coxevac® group than in the challenged control goats. Coxevac® vaccinated goats on the other hand presented an intermediate expression of these genes in our study. Thus, the QuilA® adjuvant triggered in the spleen of Coxevac® vaccinated goats a Th1-type response probably driven by $CD8^+$ and NK cells. In *C. burnetii* infection, both $CD4^+$ and $CD8^+$ T cells play a role in controlling Q Fever in mice[33,38]. However, in a mouse model, the protection induced by $CD8^+$ T cells resulted in less lung inflammation and decreased bacterial growth in spleens compared to $CD4^+$ T cell dependent-protection, suggesting that efficacious vaccines against Q Fever should elicit $CD8^+$ T-cell immunity[66]. T-cells, together with NK cells, are the major IFNɣ producers. In the murine model, NK cells did not intervene in bacterial clearance but participated in the inflammatory response against Q Fever[42]. *C. burnetii* can infect NK cells, which secrete IFNɣ and release lytic granules containing bacteria via degranulation[67]. Whether this also occurs in goats remains to be investigated. In *C. burnetii* primary infection, IFNɣ leads to apoptosis of infected macrophages and direct *C. burnetii* killing[40,68,69]. In murine models, the Th1-mediated response is involved in both primary and protective immunity. Deficient $IFN\gamma^{-/-}$ mice have a high susceptibility to NM phI infection. The infection progresses faster in $IFN\gamma^{-/-}$ mice compared to other immunodeficient animals[42]. In addition, a Th1-dominant immune response was induced following phase I and II vaccination and challenge in BALB/c mice[33]. Considering the crucial role of the IFNɣ response in *C. burnetii* infection, we further investigated the expression of IP10, a chemokine produced in response to IFN-γ. During *C. burnetii* infection, IP10 is strongly induced by IFN-γ and its expression is increased in infected mice, as a model of acute Q Fever[70–72]. By contrast, in patients with chronic Q Fever, IP10 expression is downregulated[73,74]. In our study, *IP10* was part of the transcriptional cluster which included genes more expressed in the spleen or in bronchial lymph-nodes of the QuilA®-Coxevac® group. In bronchial lymph nodes, *IP10* was grouped with *TBX21* (or T-bet), the master regulator of the Th1 differentiation program, and *TRGC2*, the receptor of γδ T cells. The role of γδ T cells during *C. burnertii* infection or protective immunity is not characterized and it is presented here in the goat challenge model for the first time. γδ T cells are distinguished by their production of IFN-γ or IL17*a*. Their effector fate is regulated by a network of transcription factors: T-bet promotes the production of IFN-γ by γδ T cells, while SOX4 and SOX13 promote IL17*a* production[75]. In our study, bronchial lymph nodes of goats vaccinated with QuilA®-Coxevac® presented an IFN-γ-mediated response (increase of *IP10*) possibly driven by γδ T cells and T-bet (increase of both *TRGC2* and *TBX21*). T-bet has been described to play a key role during *C. burnetii* primary and protective immunity. $Tbet^{-/-}$ mice experience more severe infection and a decreased ability to control bacterial replication not only after primary infection but also after vaccination-challenge[64,76].

While QuilA®-Coxevac® vaccination was associated with increase transcripts of γδ T cell receptor, T-bet and IFNγ-dependent protein, primary infection of goats was identified with a rise of SOX4/IL-17A and γδ T cell receptor transcripts, highlighting a possible role for γδ T cell subpopulations during vaccination and infection. During acute Q Fever infection, circulating γδ T cells increase in patients[77]. *In vitro* studies showed that *C. burnetii* downregulated the IL-17*a* signaling pathway in murine alveolar macrophages and that the activation of this pathway resulted in bacterial elimination[78]. On the other hand, Elliott et al.[63] demonstrated that IL17*a* is not essential during Q Fever infection. To date, the exact role of IL-17*a* producing γδ T cells in the immune response activated after *C. burnetii* infection remains to be elucidated. While in our study different γδ T cell transcript profiles were present in vaccinated vs control animals, no changes in the relative frequency of γδ T cells and $WC1^+$ γδ T were observed among conditions. This suggests that possible effects on γδ T cells due to vaccination or challenge could relate to changes in their functional role rather into their relative abundance.

To have a global view of the immune responses activated by the different conditions, we used the pattern recognition approach through the PCA. This analysis corroborated the existence of three distinct clusters with characteristics thoroughly discussed above. The use of PCA for the evaluation of vaccine-induced responses and vaccine efficacy provided an added value to our study. Overall, all data suggest that the activation of a Th1-biased response by QuilA®-Coxevac® vaccination helps the protection against *C. burnetii* infection. In contrast, the down-regulation of these pathways would be a survival strategy for the bacterium, as observed in challenged control goats which presented a different immune response.

In conclusion, this study described for the first time the immune response generated by Coxevac® vaccination in a goat model of aerosol challenge with an axenic culture of *C. burnetii* isolated from a field sample. Coxevac® did not induce a significant humoral or cellular response able to confer substantial protection upon challenge. It confirmed previous field studies showing that Coxevac® is not able to prevent Q Fever infection. Our data reconfirm the low immunogenicity of this vaccine and the need to improve its formulation by reconsidering several aspects such as the antigen, the dose or the inactivation method. Considering that the addition of QuilA® to the Coxevac® formulation increased the humoral response and elicited a sustained Th1-type cellular response, which improved vaccine efficacy, we propose to test the use of QuilA® to increase Coxevac® efficacy against *C. burnetii* infection in field settings.

MATERIALS AND METHODS

1. In vitro and *in vivo* quality controls of the bacterial inoculum

1.1 *C. burnetii* strain and culture

CbBEC2 is a Belgian strain representative of the SNP2 genomic group, isolated from infected caprine milk. The strain, initially isolated *in vivo* in BALB/c mice[79], was either (1) propagated again in BALB/c mice (Charles Rivers, Wilmington, MA, USA) (Passage P2), from now on indicated as freshly collected splenic harvest, or (2) propagated in African green monkey kidney (Vero) cells (2 passages) and then in Acidified Citrate Cysteine Medium-2 (ACCM-2)[80,81] (3 passages) (P6). The CbBEC2 strain was isolated and maintained at the National Reference Laboratory for *Coxiella burnetii* and *Bartonella* (Sciensano, Brussels, Belgium).

1.2. Analysis of *C. burnetii* LPS

The presence of a full-length lipopolysaccharide (LPS), distinctive of virulent phase I strains, was assessed in the CbBEC2 strain by whole genome sequencing (WGS) and SDS-PAGE silver staining. Genomic DNA extracted from a 14-day ACCM-2 culture (P6) was sequenced on the Illumina MiSeq platform and assembled as described[82]. To ascertain the presence of genes involved in the synthesis of a full length LPS, CbBEC2 assembly was aligned in NCBI BLASTN (Galaxy version 2.10.1) with the Nine Mile (NM) phase I sequence of the operon involved in the biosynthesis of the complete LPS (Genbank accession number: AF387640). Illustration of the alignment was obtained using the CLC sequence viewer software (Version 8.0).

C. burnetii LPS from confluent ACCM-2 cultures was extracted as previously reported[29]. LPS (6 µl, diluted 1:3) was then electrophoresed on 4–20% precast protein gels (Bio-rad, Hercules, CA, USA) together with the PageRuler prestained protein ladder (ThermoFisher Scientific, Waltham, MA USA). The gel was fixed in 25% (vol/vol) ethanol, 8% (vol/vol) acetic acid, 25% (vol/vol) formaldehyde solution (37 wt. % in H_2O). LPS was visualized using silver staining of the gel by consecutive baths of 0.8 mM

sodium thiosulfate pentahydrate, 10 nM silver nitrate, 250 nM sodium carbonate and 25 nM $Na_2EDTA.2H_2O$. Gels were imaged using a digital camera.

1.3 Analysis of the *C. burnetii* infectious potential in a mouse infection model

Six-week-old female BALB/c mice were injected intraperitoneally with 4-5x10^3 CbBEC2 *C. burnetii* cells (200 µl) derived from freshly collected splenic harvest (P2) or a 4-day old axenic ACCM-2 culture (P6). The axenic culture was arrested at the exponential phase of bacterial growth. Dilutions of *C. burnetii* from stock suspensions were obtained in 0.85% saline (Biorad). Control mice were injected with 0.85% saline only. Inocula were quantified with the monocopy *com1* real-time PCR[83]. The cycle threshold (Ct) was used to calculate the genomic equivalents (G.E.) of the suspension pondered against a calibration curve obtained with an external reference (ThermoFisher). A group of six mice was used for each strain type and for the four time-points (48 mice in total). At sacrifice, serum and spleen were collected from each animal to evaluate the serological responses (IgM and IgG), the organ weight (spleen, liver and lung) and the bacterial load (G.E. in spleen, liver and lung) as described previously[83]. The experiment, performed in BSL-3 animal facilities, received ethical approval under the file number 20160323.

2. Vaccination-challenge experiment in goats

2.1 Animals and experimental design

Sixteen 2-3 years old Saanen goats, bred from Q-fever free herds (defined as free of disease in the past 8 years by the bulk tank milk surveillance program), were tested for Q-fever, brucellosis, *Chlamydia abortus*, paratuberculosis, Schmallenberg virus, and caprine arthritis encephalitis virus. Goats were randomly distributed into three experimental groups: control (n=4), vaccine only (Coxevac® group, n=6) and vaccine plus adjuvant (QuilA®-Coxevac® group, n=6). Figure 1 shows the timeline of the vaccination-challenge experiment. After two weeks of acclimatization, goats were vaccinated subcutaneously 2 cm above the *Spina scapula* with 2 ml of Coxevac® (72 QF Units/ml, CEVA Sante Animale, Libourne, France) or with 150 µg of QuilA® (Invivogen, San Diego, CA, USA) diluted in 2 ml of Coxevac®. As controls, goats were injected with 2 ml of PBS (pH 7.4, Gibco). At 4 weeks post-vaccination (wpv), goats received a booster dose following the manufacturer's recommendations. At 13 wpv, all groups received an intranasal challenge with 10^6 CbBEC2 *C. burnetii* derived from 4-day old axenic ACCM-2 culture (P6). Inocula were diluted in 1 ml PBS and quantified with the monocopy *com1* real-time PCR. Inoculation (0.5 ml/nostril) was performed using a small nebulizer (1-mm spray opening) fixed on a syringe. Nostrils were held alternately closed during inhalation.

The general health and the rectal temperature of goats were monitored daily by clinical inspections until the end of the experiment (19 wpv). Blood was collected for serological and immunological analyses at the indicated time points (Figure 1). At the end of the study, goats were sacrificed by stunning with a penetrating captive bolt followed by immediate exsanguination. Blood and organs were collected for bacterial detection, cell phenotyping and gene expression profiling. The entire experiment, conducted in BSL-2 (vaccination) and BSL-3 (challenge) animal facilities, received ethical approval under the file numbers 20190704-01 and 20190704-02.

2.2 *C. burnetii*-specific antibody response

Total IgG antibody levels directed against *C. burnetii* (antigen Phase I + II) were measured using the commercially available PrioCHECK™ Ruminant Q fever Ab Plate Kit (Applied Biosystems; Thermo Fisher Scientific, Inc.) according to the manufacturer's instructions. Briefly, serum samples (diluted 1:400)

were added to the plate coated with *C. burnetii* whole-cell antigens and detected with the HRP-conjugated G protein at 1:100 dilution. The optical densities (OD) were measured at dual wavelengths of 450-620 nm on a microplate reader (Sunrise, Tecan Trading AG, Switzerland). S/P% > 40 was considered as positive.

2.3 IFNγ ELISA

Blood was sampled from the jugular vein on BD Vacutainer® Heparin Tubes (BD Bioscience, San Jose, CA, USA) and PBMCs were isolated using Ficoll®-Paque PREMIUM 1.073 (GE Healthcare, Chicago, IL, USA) density gradient centrifugation. After washing, PBMCs were resuspended in RPMI 1640 Medium with GlutaMAX™ (Gibco) and 10% fetal bovine serum (FBS) (Gibco) as supplement. Cells were seeded in 180 uL at $3.0x10^5$ cells/well in 96 well-plates (VWR, Radnor, PA, USA) and incubated either with 20 µL 1x PBS (Gibco), *C. burnetii* CbBEC2 inactivated antigen (2×10^7/ml) or pokeweed mitogen (PWM) at 5 µg/mL (positive control) for 48h. After centrifugation, the supernatant was harvested and stored at -20°C. IFNγ secretion was measured in the supernatant with a sandwich ELISA using the ID screen® Ruminant IFNγ kit (IDvet, Grabels, France) according to the manufacturer's instructions. Antigen-specific stimulation was validated for each time point by the positive (PWM) and negative (PBS) controls of stimulation. Recombinant goat IFNγ (Cusabio, Houston, TX, USA) was used to validate the recognition of goat IFNγ by the antibodies provided in the kit.

2.4 Isolation of splenocytes and lymph node cells

At sacrifice, spleens, bronchial and inguinal reproductive lymph nodes were aseptically removed and 1 cm^3 of tissue was disrupted and homogenized for cell isolation. After passage through 70 µM cell strainers (Corning Life Science, Corning, NY, USA), cells were suspended in RPMI 1640 medium with GlutaMAX™ (Gibco) and 10% FBS (Gibco) as supplement. Splenocytes were incubated with the BD Pharm Lyse™ lysing solution (BD Bioscience, San Jose, CA, USA), according to the manufacturer's protocol, for red blood cell lysis. Successively, splenocytes, bronchial and inguinal lymph node cells were immediately stained for cell phenotyping or cryopreserved in 90% FBS (Gibco) with 10% DMSO (Merck, Darmstadt, Germany) for further testing (RNA extraction or *C. burnetii* detection).

2.5 Immunophenotyping with flow cytometry

Isolated PBMCs, splenocytes, bronchial and inguinal lymph node cells were immediately (*ex-vivo*) stained for phenotyping using monoclonal antibodies (mAb) against CD4 (Alexa Fluor®647, clone 44.38, Bio-rad), CD8 (FITC, clone 38.65, Bio-rad) and CD21 (RPE, clone CC21, Bio-rad). Mouse IgG1-RPE (MCA928, Bio-rad) was used as isotype control. The LIVE/DEAD™ Fixable Near-IR Dead Cell Stain Kit (Invitrogen, Waltham, MA, USA) was used to stain dead cells. PBMCs cryopreserved in 90% FBS (Gibco) with 10% DMSO (Merck, Darmstadt, Germany) were stained using mAb anti-WC1 (Clone CC15, Bio-rad), anti-γδ TCR1-N24 δ chain specific (G-GB21A, Monoclonal Antibody Centre, Washington State University, Pullman, WA, USA) and the secondary antibody rabbit anti-mouse IgG-RPE (Bio-rad). The LIVE/DEAD™ Fixable Aqua Dead Cell Stain Kit (Invitrogen) determined the viability of the cells. Cells were preserved in 4% PFA (Santa Cruz Biotechnology, Dallas, TX, USA) (max. overnight) until flow cytometry was performed with BD FACSVerse™ Cytometer (BD Bioscience, San Jose, CA, USA). Data acquisition and analysis were accomplished using BD FACSuite (BD Bioscience) and FlowJo software (FlowJo, LLC, Ashland, OR, USA), respectively.

2.6 Gene expression analysis

RNA was isolated from $5x10^6$ cryopreserved splenocytes and bronchial lymph node cells using the RNeasy Mini Kit (Qiagen, Hilden, Germany), following the manufacturer's guidelines. DNA contamination was removed by treatment with the RNase-Free DNase Set (Qiagen). The concentration and purity of RNA samples was assessed using Nanodrop 1000 (Isogen Life Science, De Meern, The Netherlands) and the reverse transcription was performed on equal RNA amounts for each sample with the QuantiTect Reverse Transcription Kit (Qiagen). Gene expression was quantified by real-time PCR using the LightCycler® 480 SYBR Green I Master (Roche, Basel, Switzerland) following the manufacturer's recommendations in a Light cycler® 480 Instrument II (Roche) with cycling conditions of pre-heat (10 min at 95°C), denaturation (40 times 15 s at 95°C), annealing (40 times 1 min at 60°C). Primers (Table S1) were designed on the NCBI Primer-Blast tool (https://www.ncbi.nlm.nih.gov/tools/primer-blast/) and PCR efficiency was defined for all genes using the standard curve method. Six genes (*18S, GAPDH, HMBS, HSP90, SDHA, YWHAZ,*) were selected as possible reference genes according to the literature[9,11,84–88]. Three genes (*GAPDH, HMBS, YWHAZ* for splenocytes and *GAPDH*, *HMBS, HSP90* for bronchial lymph node cells) were selected as the most stable reference genes using geNorm NormFinder[89] and Bestkeeper[90] software packages. The relative gene expression was calculated using the model described in Hellemans et al.[91], which takes into account primer efficiency and three (or more) reference genes.

2.7 *C. burnetii* detection

The presence of *C. burnetii* was investigated in blood (post-challenge) and the organs listed in Table S2. Briefly, DNA was extracted from 200 µl of blood or homogenized tissues (max. 1 g in 1 ml MilliQ water) with the MagMax™ Isolation Kit (Applied Biosystems; Thermo Fisher Scientific, Inc.) according to the manufacturer's instructions. *C. burnetii* DNA was detected on a 7500 Real-Time PCR System (Applied Biosystems; Thermo Fisher Scientific, Inc.) by real-time PCR targeting the IS*1111* repetitive element as previously described[83].

Considering that the detection limit of the PCR assay was reached, a volume of 200 µL containing approximately $5*10^5$ frozen splenocytes and bronchial lymph nodes cells, suspended in 1x PBS (pH 7.4, Gibco), were injected into embryonated eggs (triplicates for each sample) for bacterial amplification as described[79]. The yolk sac was harvested and homogenized in 9 ml 0.85% saline. The samples (200 µl) were inactivated for 40 min at 80°C and incubated for 30 min at 37°C with 180 µl of lysis buffer (20 mM Tris pH8, 2 mM EDTA, 1.2% Triton x-100) containing 20 mg/ml lysozyme (Roche) and 4 µl of RNase A (17,500 U) (Qiagen). DNA was extracted using the QIAGEN kit DNeasy (Qiagen) according to the manufacturer's guidelines. The real-time PCR was run as described before in a Light cycler® 480 Instrument II (Roche). The cut-off for positivity was set at a Ct-value < 40 (accredited validation file). Goats presenting at least one positive result were considered to be positive.

2.8 Data analysis

General statistical analyses were performed as indicated in figure legends using GraphPad Prism Software Version 9 (San Diego, CA, USA). A p value ≤ 0.05 was considered significant.

The clustering analysis was performed in R using data issued from the gene expression profiling. Briefly, the distance matrix was calculated applying the maximum distance, the hierarchical clustering was run with the hclust function using the ward.D2 method and the dendrogram was plotted employing the ggdendro package. The heatmap was created via the ggplot2 package after data transformation with tidyverse package. Finally, the multi plot figure was constructed using the grid package.

The principal component analysis (PCA) was computed in R using the prcomp function on selected data. PCA results were extracted and visualized using the factoextra package, while the 3D visualization was performed with the scatterplot3D package.

ACKNOWLEDGMENTS

The authors acknowledge the interesting and fruitful discussions within the Vetimmune initiative (Sciensano), as well as the precious advices from Prof. B. Goddeeris (KU Leuven), Prof. C.L. Baldwin (University of Massachusetts), and Prof. P.A. Beare (NIH). Gratitude is also due to T. Fancello for his important technical assistance, always responding to the variegate demands. The authors thank (listed in alphabetical order) R. Bakinahe Ntamukunzi, D. Desqueper, P. Michel, M. Rhabi, A. Soares and P. Vanoorenberghe for their excellent technical support. Hence, gratefulness is devoted to B. De Bock, W. Van Campe, A. Bouquiaux, L. Mostin and all the colleagues from the experimental centre in Machelen (Sciensano).

AUTHOR CONTRIBUTIONS

Conceptualization: M. Mori, W. Jansen, S. Tomaiuolo; methodology: M. Mori, W. Jansen, S. Tomaiuolo, B. Devriendt, E. Cox; software: S. Tomaiuolo, S.S. Martins; formal analysis: S. Tomaiuolo, S.S. Martins; investigation: W. Jansen, S. Tomaiuolo, S.S. Martins, M.Mori; data curation: S. Tomaiuolo, M.Mori; writing—original draft preparation: S. Tomaiuolo; writing—review and editing: S. Tomaiuolo, M.Mori, B. Devriendt, W. Jansen, E.Cox; supervision: M.Mori, B. Devriendt, E.Cox; project administration and funding acquisition: M.Mori.

FUNDING

S. Tomaiuolo is supported by the NRC grant, financed by the Belgian Ministry of Social Affairs through a fund of the Health Insurance System. This work was partly supported by Sciensano through the internal project VETIMMUNE.

CONFLICT OF INTEREST

The authors declare that the research was conducted in the absence of any commercial or financial relationships that could be construed as a potential conflict of interest.

REFERENCES

1. Oyston, P. C. F. & Davies, C. Q fever: the neglected biothreat agent. *J Med Microbiol* **60**, 9–21 (2011).
2. Sanford, S. E., Josephson, G. K. & MacDonald, A. Coxiella burnetii (Q fever) abortion storms in goat herds after attendance at an annual fair. *Can Vet J* **35**, 376–378 (1994).
3. Emery, M. P. *et al.* Coxiella burnetii serology assays in goat abortion storm. *J Vet Diagn Invest* **26**, 141–145 (2014).
4. Guatteo, R., Beaudeau, F., Joly, A. & Seegers, H. Coxiella burnetii shedding by dairy cows. *Vet Res* **38**, 849–860 (2007).

5. Rodolakis, A. *et al.* Comparison of Coxiella burnetii shedding in milk of dairy bovine, caprine, and ovine herds. *J Dairy Sci* **90**, 5352–5360 (2007).
6. Maurin, M. & Raoult, D. Q fever. *Clin Microbiol Rev* **12**, 518–553 (1999).
7. Sánchez, J. *et al.* Experimental Coxiella burnetii infection in pregnant goats: a histopathological and immunohistochemical study. *J Comp Pathol* **135**, 108–115 (2006).
8. Roest, H.-J. *et al.* Q fever in pregnant goats: pathogenesis and excretion of Coxiella burnetii. *PLoS One* **7**, e48949 (2012).
9. Roest, H. I., Post, J., van Gelderen, B., van Zijderveld, F. G. & Rebel, J. M. Q fever in pregnant goats: humoral and cellular immune responses. *Veterinary Research* **44**, 67 (2013).
10. Roest, H. I. J., Dinkla, A., Koets, A. P., Post, J. & van Keulen, L. Experimental Coxiella burnetii infection in non-pregnant goats and the effect of breeding. *Vet Res* **51**, 74 (2020).
11. Ammerdorffer, A. *et al.* The Effect of C. burnetii Infection on the Cytokine Response of PBMCs from Pregnant Goats. *PLOS ONE* **9**, e109283 (2014).
12. Achard, D. & Rodolakis, A. Q fever vaccination in ruminants: A critical review. in *The Principles and Practice of Q Fever: The One Health Paradigm* 367–389 (2017).
13. Arricau-Bouvery, N. *et al.* Effect of vaccination with phase I and phase II Coxiella burnetii vaccines in pregnant goats. *Vaccine* **23**, 4392–4402 (2005).
14. Hogerwerf, L. *et al.* Reduction of Coxiella burnetii prevalence by vaccination of goats and sheep, The Netherlands. *Emerg Infect Dis* **17**, 379–386 (2011).
15. de Cremoux, R. *et al.* Assessment of vaccination by a phase I Coxiella burnetii-inactivated vaccine in goat herds in clinical Q fever situation. *FEMS Immunol Med Microbiol* **64**, 104–106 (2012).

16. Muleme, M. *et al.* A longitudinal study of serological responses to Coxiella burnetii and shedding at kidding among intensively-managed goats supports early use of vaccines. *Vet Res* **48**, 50 (2017).

17. Rousset, E. *et al.* Efficiency of a phase 1 vaccine for the reduction of vaginal Coxiella burnetii shedding in a clinically affected goat herd. *Clin Microbiol Infect* **15 Suppl 2**, 188–189 (2009).

18. Astobiza, I. *et al.* Coxiella burnetii shedding and environmental contamination at lambing in two highly naturally-infected dairy sheep flocks after vaccination. *Res Vet Sci* **91**, e58-63 (2011).

19. Jansen, W. *et al.* Belgian bulk tank milk surveillance program reveals the impact of a continuous vaccination protocol for small ruminants against Coxiella burnetii. *Transbound Emerg Dis* (2021) doi:10.1111/tbed.14273.

20. Bauer, B. U. *et al.* Humoral immune response to Q fever vaccination of three sheep flocks naturally pre-infected with Coxiella burnetii. *Vaccine* **39**, 1499–1507 (2021).

21. Coffman, R. L., Sher, A. & Seder, R. A. Vaccine adjuvants: putting innate immunity to work. *Immunity* **33**, 492–503 (2010).

22. Katayama, S., Oda, K., Ohgitani, T., Hirahara, T. & Shimizu, Y. Influence of antigenic forms and adjuvants on the IgG subclass antibody response to Aujeszky's disease virus in mice. *Vaccine* **17**, 2733–2739 (1999).

23. Borja-Cabrera, G. P. *et al.* Effective immunotherapy against canine visceral leishmaniasis with the FML-vaccine. *Vaccine* **22**, 2234–2243 (2004).

24. Haçariz, O. *et al.* The effect of Quil A adjuvant on the course of experimental Fasciola hepatica infection in sheep. *Vaccine* **27**, 45–50 (2009).

25. Sun, H.-X., Xie, Y. & Ye, Y.-P. Advances in saponin-based adjuvants. *Vaccine* **27**, 1787–1796 (2009).

26. Villa-Mancera, A., Reynoso-Palomar, A., Utrera-Quintana, F. & Carreón-Luna, L. Cathepsin L1 mimotopes with adjuvant Quil A induces a Th1/Th2 immune response and confers significant protection against Fasciola hepatica infection in goats. *Parasitol Res* **113**, 243–250 (2014).

27. Rahman, M. *et al.* QuilA-Adjuvanted T. gondii Lysate Antigens Trigger Robust Antibody and IFNγ+ T Cell Responses in Pigs Leading to Reduction in Parasite DNA in Tissues Upon Challenge Infection. *Front Immunol* **10**, 2223 (2019).

28. Narasaki, C. T. & Toman, R. Lipopolysaccharide of Coxiella burnetii. *Adv Exp Med Biol* **984**, 65–90 (2012).

29. Beare, P. A., Jeffrey, B. M., Long, C. M., Martens, C. M. & Heinzen, R. A. Genetic mechanisms of Coxiella burnetii lipopolysaccharide phase variation. *PLoS Pathog* **14**, e1006922 (2018).

30. Beare, P. A. *et al.* Genetic diversity of the Q fever agent, Coxiella burnetii, assessed by microarray-based whole-genome comparisons. *J Bacteriol* **188**, 2309–2324 (2006).

31. Kishimoto, R. A., Rozmiarek, H. & Larson, E. W. Experimental Q fever infection in congenitally athymic nude mice. *Infect Immun* **22**, 69–71 (1978).

32. Guigno, D. *et al.* Primary humoral antibody response to Coxiella burnetii, the causative agent of Q fever. *J Clin Microbiol* **30**, 1958–1967 (1992).

33. Zhang, G. *et al.* Mechanisms of Vaccine-Induced Protective Immunity against Coxiella burnetii Infection in BALB/c Mice. *The Journal of Immunology* **179**, 8372–8380 (2007).

34. Singh, M. & O'Hagan, D. T. Recent advances in veterinary vaccine adjuvants. *Int J Parasitol* **33**, 469–478 (2003).

35. Cox, E., Verdonck, F., Vanrompay, D. & Goddeeris, B. Adjuvants modulating mucosal immune responses or directing systemic responses towards the mucosa. *Vet Res* **37**, 511–539 (2006).

36. Burakova, Y., Madera, R., McVey, S., Schlup, J. R. & Shi, J. Adjuvants for Animal Vaccines. *Viral Immunol* **31**, 11–22 (2018).

37. Sander, V. A., Corigliano, M. G. & Clemente, M. Promising Plant-Derived Adjuvants in the Development of Coccidial Vaccines. *Front Vet Sci* **6**, 20 (2019).

38. Kumaresan, V., Alam, S., Zhang, Y. & Zhang, G. The Feasibility of Using Coxiella burnetii Avirulent Nine Mile Phase II Viable Bacteria as a Live Attenuated Vaccine Against Q fever. *Front Immunol* **12**, 754690 (2021).

39. Turco, J., Thompson, H. A. & Winkler, H. H. Interferon-gamma inhibits growth of Coxiella burnetii in mouse fibroblasts. *Infect Immun* **45**, 781–783 (1984).

40. Dellacasagrande, J., Capo, C., Raoult, D. & Mege, J. L. IFN-gamma-mediated control of Coxiella burnetii survival in monocytes: the role of cell apoptosis and TNF. *J Immunol* **162**, 2259–2265 (1999).

41. Howe, D., Barrows, L. F., Lindstrom, N. M. & Heinzen, R. A. Nitric oxide inhibits Coxiella burnetii replication and parasitophorous vacuole maturation. *Infect Immun* **70**, 5140–5147 (2002).

42. Andoh, M. *et al.* T cells are essential for bacterial clearance, and gamma interferon, tumor necrosis factor alpha, and B cells are crucial for disease development in Coxiella burnetii infection in mice. *Infect Immun* **75**, 3245–3255 (2007).

43. Zamboni, D. S. & Rabinovitch, M. Nitric oxide partially controls Coxiella burnetii phase II infection in mouse primary macrophages. *Infect Immun* **71**, 1225–1233 (2003).

44. Marciani, D. J. Vaccine adjuvants: role and mechanisms of action in vaccine immunogenicity. *Drug Discov Today* **8**, 934–943 (2003).

45. Maraskovsky, E. *et al.* Development of prophylactic and therapeutic vaccines using the ISCOMATRIX adjuvant. *Immunol Cell Biol* **87**, 371–376 (2009).

46. Cibulski, S. P. *et al.* Novel ISCOMs from Quillaja brasiliensis saponins induce mucosal and systemic antibody production, T-cell responses and improved antigen uptake. *Vaccine* **34**, 1162–1171 (2016).

47. Lacaille-Dubois, M.-A. Updated insights into the mechanism of action and clinical profile of the immunoadjuvant QS-21: A review. *Phytomedicine* **60**, 152905 (2019).

48. Marciani, D. J. Elucidating the Mechanisms of Action of Saponin-Derived Adjuvants. *Trends Pharmacol Sci* **39**, 573–585 (2018).

49. Cowley, S. C. *et al.* CD4−CD8− T cells control intracellular bacterial infections both in vitro and in vivo. *J Exp Med* **202**, 309–319 (2005).

50. Raju Paul, S. *et al.* Natural Exposure- and Vaccination-Induced Profiles of Ex Vivo Whole Blood Cytokine Responses to Coxiella burnetii. *Front Immunol* **13**, 886698 (2022).

51. Capo, C. *et al.* Upregulation of tumor necrosis factor alpha and interleukin-1 beta in Q fever endocarditis. *Infect Immun* **64**, 1638–1642 (1996).

52. Honstettre, A. *et al.* Dysregulation of Cytokines in Acute Q Fever: Role of Interleukin-10 and Tumor Necrosis Factor in Chronic Evolution of Q Fever. *The Journal of Infectious Diseases* **187**, 956–962 (2003).

53. Kremers, M. N. T. *et al.* Correlations between peripheral blood Coxiella burnetii DNA load, interleukin-6 levels, and C-reactive protein levels in patients with acute Q fever. *Clin Vaccine Immunol* **21**, 484–487 (2014).

54. Penttila, I. A. *et al.* Cytokine dysregulation in the post-Q-fever fatigue syndrome. *QJM* **91**, 549–560 (1998).

55. Ghigo, E., Capo, C., Raoult, D. & Mege, J.-L. Interleukin-10 Stimulates Coxiella burnetii Replication in Human Monocytes through Tumor Necrosis Factor Down-Modulation: Role in Microbicidal Defect of Q Fever. *Infect Immun* **69**, 2345–2352 (2001).

56. Ghigo, E. *et al.* Link between Impaired Maturation of Phagosomes and Defective Coxiella burnetii Killing in Patients with Chronic Q Fever. *The Journal of Infectious Diseases* **190**, 1767–1772 (2004).

57. Meghari, S. *et al.* Persistent Coxiella burnetii Infection in Mice Overexpressing IL-10: An Efficient Model for Chronic Q Fever Pathogenesis. *PLOS Pathogens* **4**, e23 (2008).

58. Ghigo, E., Imbert, G., Capo, C., Raoult, D. & Mege, J.-L. Interleukin-4 Induces Coxiella burnetii Replication in Human Monocytes but not in Macrophages. *Annals of the New York Academy of Sciences* **990**, 450–459 (2003).

59. Mantovani, A. *et al.* The chemokine system in diverse forms of macrophage activation and polarization. *Trends Immunol* **25**, 677–686 (2004).

60. Benoit, M., Barbarat, B., Bernard, A., Olive, D. & Mege, J.-L. Coxiella burnetii, the agent of Q fever, stimulates an atypical M2 activation program in human macrophages. *European Journal of Immunology* **38**, 1065–1070 (2008).

61. Gilkes, A. P. *et al.* Tuning Subunit Vaccines with Novel TLR Triagonist Adjuvants to Generate Protective Immune Responses against *Coxiella burnetii*. *J.I.* **204**, 611–621 (2020).

62. Long, C. M. Q Fever Vaccine Development: Current Strategies and Future Considerations. *Pathogens* **10**, 1223 (2021).

63. Elliott, A., Schoenlaub, L., Freches, D., Mitchell, W. & Zhang, G. Neutrophils Play an Important Role in Protective Immunity against Coxiella burnetii Infection. *Infect Immun* **83**, 3104–3113 (2015).

64. Ledbetter, L., Cherla, R., Chambers, C., Zhang, Y. & Zhang, G. Eosinophils Affect Antibody Isotype Switching and May Partially Contribute to Early Vaccine-Induced Immunity against Coxiella burnetii. *Infect Immun* **87**, e00376-19 (2019).

65. Kumaresan, V. *et al.* Coxiella burnetii Virulent Phase I and Avirulent Phase II Variants Differentially Manipulate Autophagy Pathway in Neutrophils. *Infect Immun* **90**, e0053421 (2022).

66. Read, A. J., Erickson, S. & Harmsen, A. G. Role of CD4+ and CD8+ T cells in clearance of primary pulmonary infection with Coxiella burnetii. *Infect Immun* **78**, 3019–3026 (2010).

67. Matthiesen, S. *et al.* Coxiella burnetii-Infected NK Cells Release Infectious Bacteria by Degranulation. *Infect Immun* **88**, e00172-20 (2020).

68. Dellacasagrande, J., Ghigo, E., Raoult, D., Capo, C. & Mege, J.-L. IFN-γ-Induced Apoptosis and Microbicidal Activity in Monocytes Harboring the Intracellular Bacterium Coxiella burnetii Require Membrane TNF and Homotypic Cell Adherence. *The Journal of Immunology* **169**, 6309–6315 (2002).

69. Capo, C. & Mege, J.-L. Role of innate and adaptive immunity in the control of Q fever. *Adv Exp Med Biol* **984**, 273–286 (2012).

70. Leone, M. *et al.* Coxiella burnetii infection in C57BL/6 mice aged 1 or 14 months. *FEMS Immunology & Medical Microbiology* **50**, 396–400 (2007).

71. Schoffelen, T. *et al.* Early cytokine and antibody responses against Coxiella burnetii in aerosol infection of BALB/c mice. *Diagnostic Microbiology and Infectious Disease* **81**, 234–239 (2015).

72. Kohl, L. *et al.* MyD88 Is Required for Efficient Control of Coxiella burnetii Infection and Dissemination. *Frontiers in Immunology* **10**, (2019).

73. Pennings, J. L. A. *et al.* Dysregulation of serum gamma interferon levels in vascular chronic Q Fever patients provides insights into disease pathogenesis. *Clin Vaccine Immunol* **22**, 664–671 (2015).

74. Raijmakers, R. P. H. *et al.* A possible link between recurrent upper respiratory tract infections and lower cytokine production in patients with Q fever fatigue syndrome. *European Journal of Immunology* **49**, 1015–1022 (2019).

75. Parker, M. E. & Ciofani, M. Regulation of γδ T Cell Effector Diversification in the Thymus. *Frontiers in Immunology* **11**, (2020).

76. Mezouar, S. *et al.* T-Bet Controls Susceptibility of Mice to Coxiella burnetii Infection. *Frontiers in Microbiology* **11**, (2020).

77. Schneider, T. *et al.* The number and proportion of Vgamma9 Vdelta2 T cells rise significantly in the peripheral blood of patients after the onset of acute Coxiella burnetii infection. *Clin Infect Dis* **24**, 261–264 (1997).

78. Clemente, T. M. *et al.* Coxiella burnetii Blocks Intracellular Interleukin-17 Signaling in Macrophages. *Infect Immun* **86**, e00532-18 (2018).

79. Mori, M., Mertens, K., Cutler, S. J. & Santos, A. S. Critical Aspects for Detection of Coxiella burnetii. *Vector Borne Zoonotic Dis* **17**, 33–41 (2017).

80. Omsland, A., Cockrell, D. C., Fischer, E. R. & Heinzen, R. A. Sustained axenic metabolic activity by the obligate intracellular bacterium Coxiella burnetii. *J Bacteriol* **190**, 3203–3212 (2008).

81. Omsland, A. *et al.* Host cell-free growth of the Q fever bacterium Coxiella burnetii. *Proc Natl Acad Sci U S A* **106**, 4430–4434 (2009).

82. Tomaiuolo, S. *et al.* Phylogeography of Human and Animal Coxiella burnetii Strains: Genetic Fingerprinting of Q Fever in Belgium. *Front Cell Infect Microbiol* **10**, 625576 (2020).

83. Mori, M. *et al.* In vitro and in vivo infectious potential of coxiella burnetii: a study on Belgian livestock isolates. *PLoS One* **8**, e67622 (2013).

84. Najafpanah, M. J., Sadeghi, M. & Bakhtiarizadeh, M. R. Reference genes selection for quantitative real-time PCR using RankAggreg method in different tissues of Capra hircus. *PLoS One* **8**, e83041 (2013).

85. Zhang, Y. *et al.* Reference gene screening for analyzing gene expression across goat tissue. *Asian-Australas J Anim Sci* **26**, 1665–1671 (2013).

86. Manjunath, S. *et al.* Identification of suitable reference gene in goat peripheral blood mononuclear cells (PBMCs) infected with peste des petits ruminants virus (PPRV). *Livestock Science* **181**, 150–155 (2015).

87. Puech, C., Dedieu, L., Chantal, I. & Rodrigues, V. Design and evaluation of a unique SYBR Green real-time RT-PCR assay for quantification of five major cytokines in cattle, sheep and goats. *BMC Vet Res* **11**, 65 (2015).

88. Sahu, A. R. *et al.* Selection and validation of suitable reference genes for qPCR gene expression analysis in goats and sheep under Peste des petits ruminants virus (PPRV), lineage IV infection. *Sci Rep* **8**, 15969 (2018).

89. Pfaffl, M. W., Tichopad, A., Prgomet, C. & Neuvians, T. P. Determination of stable housekeeping genes, differentially regulated target genes and sample integrity: BestKeeper--Excel-based tool using pair-wise correlations. *Biotechnol Lett* **26**, 509–515 (2004).

90. Andersen, C. L., Jensen, J. L. & Ørntoft, T. F. Normalization of real-time quantitative reverse transcription-PCR data: a model-based variance estimation approach to identify genes suited for normalization, applied to bladder and colon cancer data sets. *Cancer Res* **64**, 5245–5250 (2004).

91. Hellemans, J., Mortier, G., De Paepe, A., Speleman, F. & Vandesompele, J. qBase relative quantification framework and software for management and automated analysis of real-time quantitative PCR data. *Genome Biol* **8**, R19 (2007).

FIGURE LEGENDS

Figure 1. Design of the vaccination and challenge experiment. A prime–boost strategy was used for the vaccination of goats with Coxevac® (n=6) or QuilA-Coxevac® (n=6). As controls, goats (n=4) were similarly injected with PBS. At week 13 post vaccination, all groups were intranasally challenged with the C. burnetii CbBEC2 strain. At the indicated time points, serum was collected to evaluate the specific antibody response, PBMCs (peripheral blood mononuclear cells) were isolated for T and B cell phenotyping and the IFNɣ (interferonɣ) production was detected in antigen stimulated PBMCs. At sacrifice, organs were collected for bacterial detection, cell phenotyping and gene expression profiling.

Figure 2. In vitro and in vivo (mice) quality controls of the bacterial inoculum. **(a)** *C. burnetii* CbBEC2 strain bears Phase I LPS as shown by the alignment of CbBEC2 contig 11 (54529 bp), extracted from the CbBEC2 assembly, and the NM phI sequence of the operon involved in the biosynthesis of the complete LPS (38584 bp). Consensus (in grey) represents the consensus sequence resulting from the alignment. Conservation (in red) shows the conservation level for each position in the alignment. The height of the bar displays the percentage of conservation for each position that in this case can oscillate between 50% (the position is present in one input sequence) and 100% (the position is present in both input sequences). **(b)** SDS-PAGE silver staining of CbBEC2 LPS at the cumulative passage 6 (P6) cultivated for 14 days in ACCM-2 and Nine Mile phase 1 LPS (**c**) Comparison of the proliferative capacity of CbBEC2 strain from freshly collected splenic harvest at P2 and that from the axenic culture at P6 in the Balb/c model at 4 time points post infection. The axenic culture triggered significantly higher bacterial loads than the P2 in the spleen when comparing the mean of the 4 time points for each group using the Mann Whitney test (*P ≤ 0.05). Data are represented as boxplots. GE/g = Genome equivalents/gram, W= week after infection.

Figure 3. QuilA®-Coxevac® prime vaccination induces a transient increase in the rectal temperature. (a) Daily monitoring of rectal temperature upon vaccination and challenge for the Control, Coxevac® and QuilA®-Coxevac® groups. **(b)** Zoom on selected time points for each group to display specific patterns of goats. Individual daily values are represented for all animals (a-b). W= week after vaccination, C= control goat, V= vaccinated goat (Coxevac®), VA= vaccinated plus adjuvant goat (QuilA®-Coxevac®).

Figure 4. Kinetics of antigen specific-IgG and IFNɣ production upon vaccination and challenge infection. (a) QuilA®-Coxevac® vaccination induced robust and sustained *C. burnetii*-specific serum IgG titers compared to the Control and Coxevac® group. Boxplots represent IgG titers calculated as the percentage of sample/positive (S/P%) ratio for each sample. S/P% > 40 was considered as positive. The antibody response was analyzed after vaccination with a multiple unpaired T test with Welch correction followed by a two-stage linear step-up method of Benjamini, Krieger and Yekutieli to correct for multiple comparisons by False Discovery Rate (FDR) (red asterisks, *FDR ≤ 0.01). After challenge, differences between the three groups were assessed using the Kruskal-Wallis test with Dunn's multiple comparison post-hoc test (black asterisks, *P ≤ 0.05; **P ≤ 0.01; ***P ≤ 0.001). **(b)** Frequency of anti-*C. burnetii* IgG titers for the Control, Coxevac® and QuilA®-Coxevac® group. Neg = Titers ≤ 40; + = 40 < titers ≤ 100; ++ = 100 < titers ≤ 200; +++ = 200 < titers ≤ 300. **(c)** Differential IFNγ secretion by PBMCs stimulated with inactivated whole cell *C. burnetii*. The IFNγ response was analyzed after challenge using mixed-effects models with Geisser-Greenhouse correction (data presented in the result section).

IFNγ secretion trends (in black) were visualized via interpolation of cubic splines. ↑= Moment of challenge.

Figure 5. The two Coxevac® formulations activate cell subsets of different nature upon challenge. (a) Gating strategy used in the analysis of T and B lymphocytes in ex-vivo stained PMBCs. Cellular subtypes were identified based on the expression of CD4, CD8 and CD21 cell markers. Plots are from a representative animal. Cell frequencies were calculated as percent of the viable cell population. **(b)** Kinetics of CD4+, CD8+, CD4-CD8- and CD21 cell frequencies in PBMCs upon vaccination and challenge. Each kinetic was analyzed using the mixed-effects models, both after vaccination and challenge, with Geisser-Greenhouse correction followed by Tukey's multiple comparison post-hoc test (*P ≤ 0.05). Data are represented as boxplots. w = week after vaccination.

Figure 6. Higher frequencies of CD8+ cells and granulocytes detected in the spleen of the QuilA®-Coxevac® group at sacrifice. (a) Frequencies of CD4+, CD8+, CD4-CD8- and CD21+ cells present in the spleen of Control, Coxevac® and QuilA®-Coxevac® goats. The gating strategy is shown in Figure 5A. **(b)** Gating strategy used in the analysis of granulocytes observed in goat spleens and quantification of their frequency. The granulocyte population was identified based on size and granularity characteristics. Group comparisons were performed using One-way ANOVA test with Tukey's multiple comparison post-hoc test (*P ≤ 0.05; **P ≤ 0.01; ***P ≤ 0.001) (a-b). Cell frequencies were calculated as percent of the viable cell population and data are represented as boxplots (a-b).

Figure 7. Distinctive transcriptional patterns are induced in spleens of vaccinated and control animals upon challenge. (a) Expression profiles of selected genes (n= 23) in control, Coxevac® and QuilA®-Coxevac® groups at sacrifice. Data are represented as scatter dot plots with a line at the geometric mean. Outliers are identified and removed using the ROUT method (Q=1%). Differences between experimental groups were tested using the One way ANOVA test with Tukey's multiple comparison post-hoc test or the Kruskal-Wallis test with Dunn's multiple comparison post-hoc test depending on the results of the homogeneity of variance and normality of residuals evaluated via the Bartlett's and Shapiro Wilk tests, respectively (*P ≤ 0.05; **P ≤ 0.01; ***P ≤ 0.001). **(b)** Hierarchical clustering heatmap analysis of data issued from the gene expression profiling in spleen. Each colored cell on the map corresponds to the value of the geometric mean for each group. Values are measured by maximum distance with a Ward.2 clustering algorithm.

Figure 8. Distinctive transcriptional patterns are induced in bronchial lymph nodes of vaccinated and control animals upon challenge. (a) Expression profiles of selected genes in control, Coxevac® and QuilA®-Coxevac® groups at sacrifice. Data are represented as scatter dot plots with a line at the geometric mean. Outliers are identified and removed using the ROUT method (Q=1%). Differences between experimental groups were tested using the One way ANOVA test with Tukey's multiple comparison post-hoc test or the Kruskal-Wallis test with Dunn's multiple comparison post-hoc test depending on the results of the homogeneity of variance and normality of residuals evaluated via the Bartlett's and Shapiro Wilk tests, respectively (*P ≤ 0.05; **P ≤ 0.01; ***P ≤ 0.001). **(b)** Hierarchical clustering heatmap analysis of data issued from the gene expression profiling in respiratory lymph nodes. Each colored cell on the map corresponds to the value of the geometric mean for each group. Values are measured by maximum distance with a Ward.2 clustering algorithm.

Figure 9. Specific immune responses distinguish Coxevac®, QuilA®-Coxevac® and control goats following *C. burnetii* challenge. (a) Principal component analysis (PCA) of the complete dataset (n = 68), which included data from serology (weeks 13.5, 17.5 and 19 pv), IFNɣ secretion upon antigen specific stimulated PBMCs (weeks 13.5, 17.5 and 19 pv), organ and blood (week 19 pv) phenotyping and gene expression profiles. **(b)** PCA of specific selected variables (n= 22) resulting in an accurate

separation of the three conditions. From the left, graph 1 is the 2D PCA score plot of the first two components (a-b). Symbols represent animals, the central one corresponds to the mean coordinates of the individuals in the group. Graph 2 is the PCA loading plot showing the distribution of all 22 variables (b) or of variables with a contribution > than 1.5 (n = 31, the loading plot containing all 68 variables is showed in Figure S4) (a). Graph 3 is the 3D PCA score plot of the first three components, realized to increase the proportion of variance illustrated by the analysis (a-b). CD4CD8 = CD4- CD8-, B = blood, S = spleen, BL= bronchial lymph nodes, RL= reproductive lymph nodes, PH = phenotyping, W= week, Contrib = contribution.

TABLE

Table 1. *C. burnetii* detection by PCR assay in splenocytes and bronchial lymph node cells isolated at sacrifice. Samples were injected in embryonated eggs (in triplicates) for bacterial amplification and only yolk sacs of eggs dying after day 5 post injection were collected (pi). V2 splenocytes and V2 and V3 respiratory lymph node cells were highly contaminated and amplification in eggs was not possible. Goats presenting at least one positive result per organ were considered to be positive.

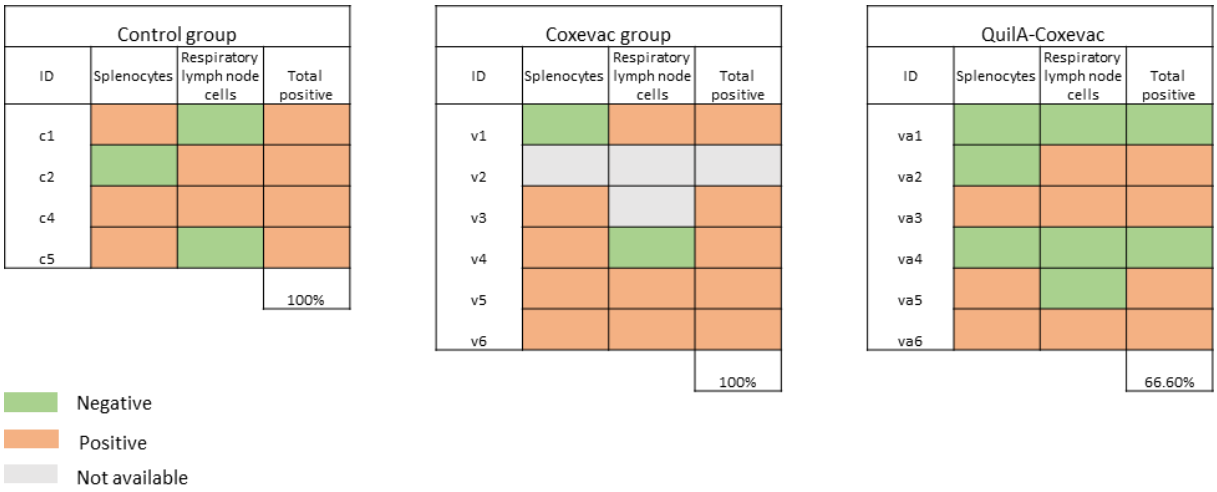

Figures

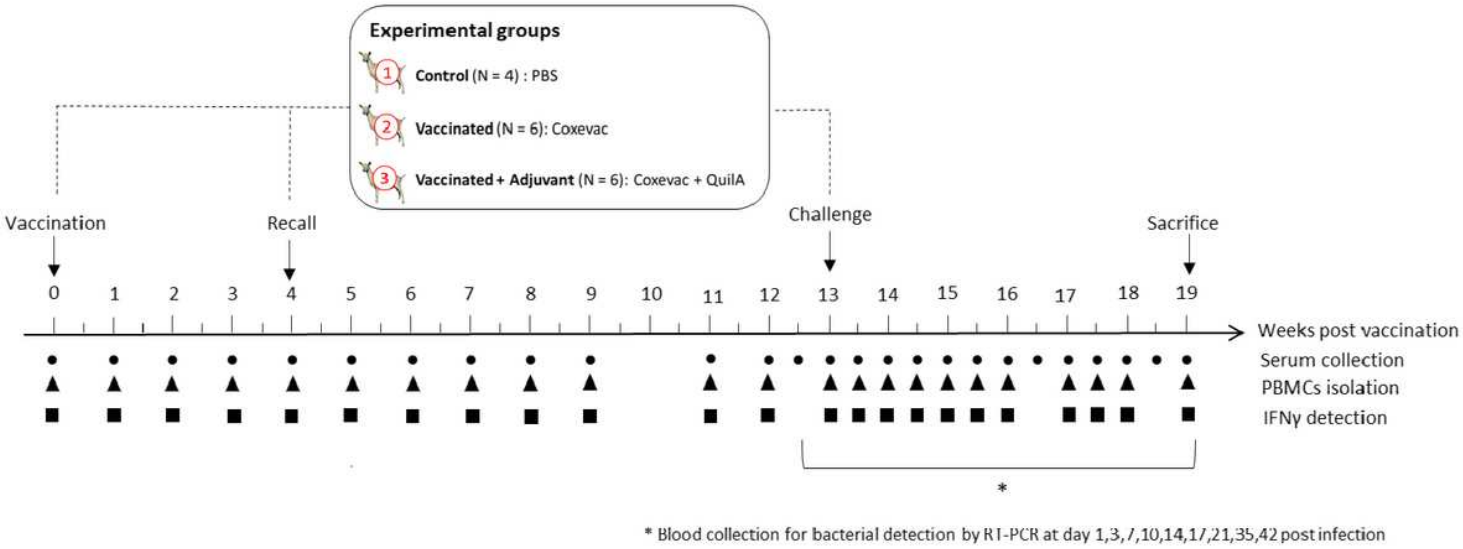

Figure 1

Design of the vaccination and challenge experiment. A prime–boost strategy was used for the vaccination of goats with Coxevac® (n=6) or QuilA-Coxevac® (n=6). As controls, goats (n=4) were similarly injected with PBS. At week 13 post vaccination, all groups were intranasally challenged with the C. burnetii CbBEC2 strain. At the indicated time points, serum was collected to evaluate the specific antibody response, PBMCs (peripheral blood mononuclear cells) were isolated for T and B cell

phenotyping and the IFN (interferon) production was detected in antigen stimulated PBMCs. At sacrifice, organs were collected for bacterial detection, cell phenotyping and gene expression profiling.

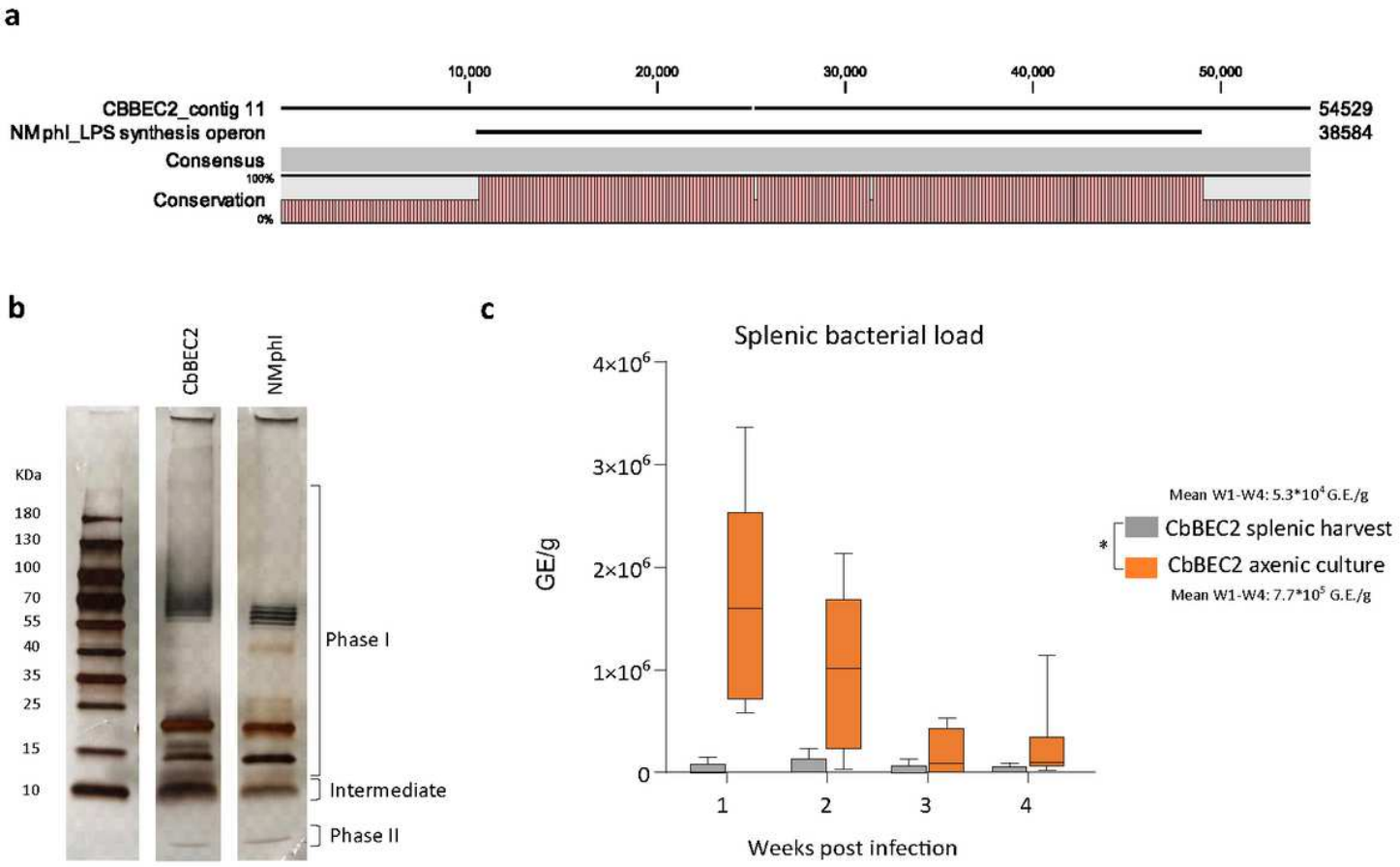

Figure 2

In vitro and in vivo (mice) quality controls of the bacterial inoculum. (a) C. burnetii CbBEC2 strain bears Phase I LPS as shown by the alignment of CbBEC2 contig 11 (54529 bp), extracted from the CbBEC2 assembly, and the NM phI sequence of the operon involved in the biosynthesis of the complete LPS (38584 bp). Consensus (in grey) represents the consensus sequence resulting from the alignment. Conservation (in red) shows the conservation level for each position in the alignment. The height of the bar displays the percentage of conservation for each position that in this case can oscillate between 50% (the position is present in one input sequence) and 100% (the position is present in both input sequences). (b) SDS-PAGE silver staining of CbBEC2 LPS at the cumulative passage 6 (P6) cultivated for 14 days in ACCM-2 and Nine Mile phase 1 LPS (c) Comparison of the proliferative capacity of CbBEC2 strain from freshly collected splenic harvest at P2 and that from the axenic culture at P6 in the Balb/c

model at 4 time points post infection. The axenic culture triggered significantly higher bacterial loads than the P2 in the spleen when comparing the mean of the 4 time points for each group using the Mann Whitney test (*P ≤ 0.05). Data are represented as boxplots. GE/g = Genome equivalents/gram, W= week after infection.

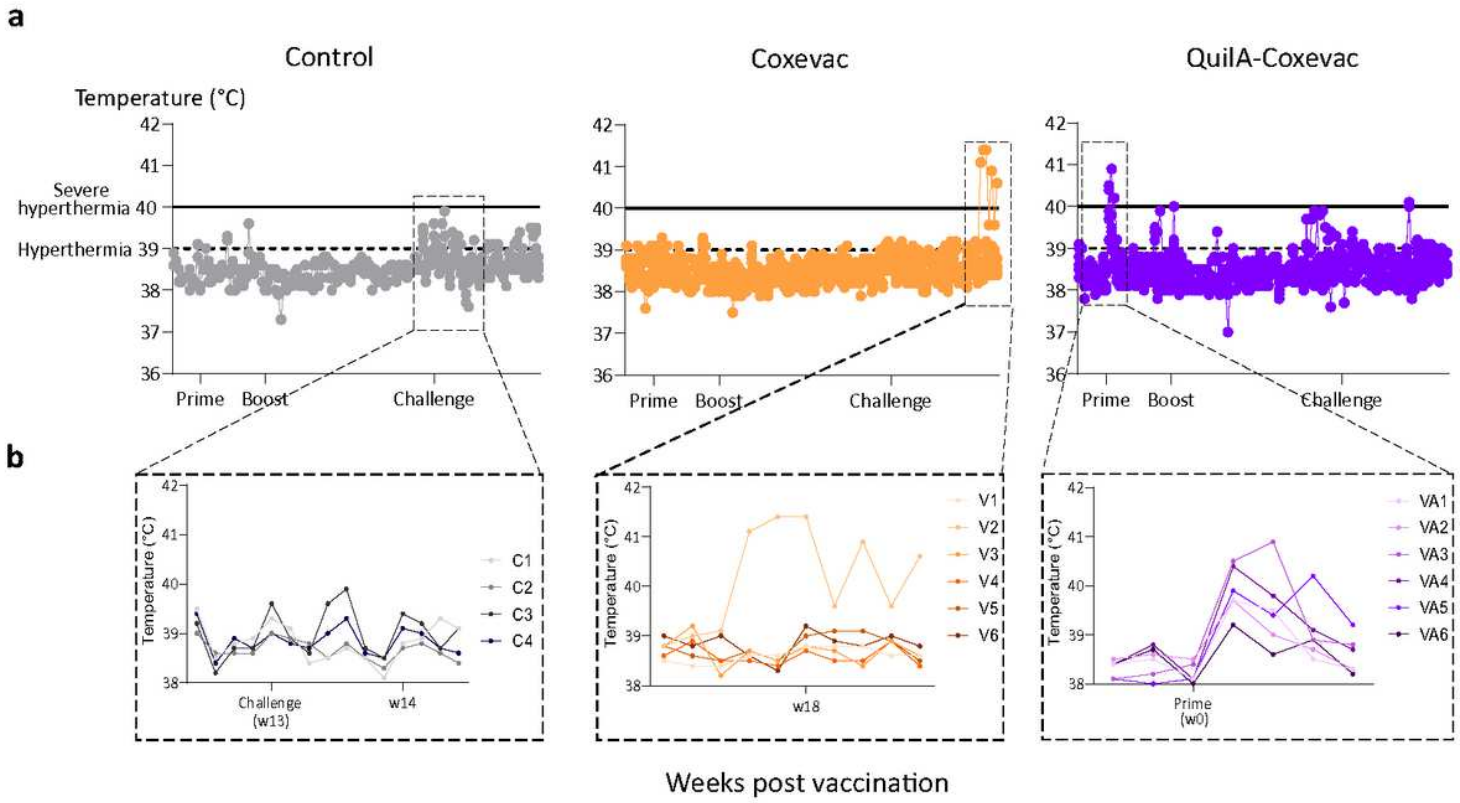

Figure 3

QuilA®-Coxevac® prime vaccination induces a transient increase in the rectal temperature. (a) Daily monitoring of rectal temperature upon vaccination and challenge for the Control, Coxevac® and QuilA®-Coxevac® groups. (b) Zoom on selected time points for each group to display specific patterns of goats. Individual daily values are represented for all animals (a-b). W= week after vaccination, C= control goat, V= vaccinated goat (Coxevac®), VA= vaccinated plus adjuvant goat (QuilA®-Coxevac®).

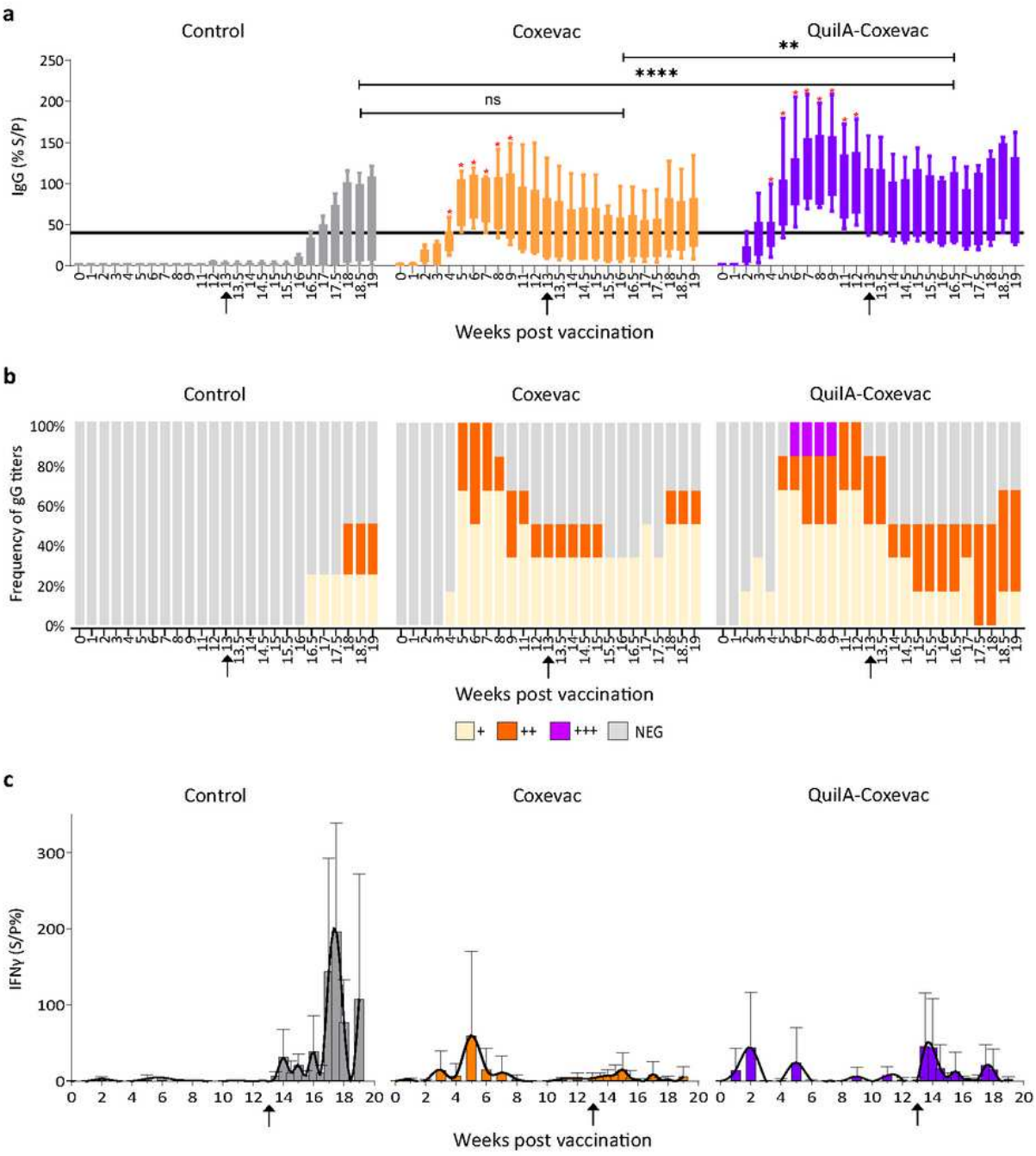

Figure 4

Kinetics of antigen specific-IgG and IFN production upon vaccination and challenge infection. (a) QuilA®-Coxevac® vaccination induced robust and sustained C. burnetii-specific serum IgG titers compared to the Control and Coxevac® group. Boxplots represent IgG titers calculated as the percentage of sample/positive (S/P%) ratio for each sample. S/P% > 40 was considered as positive. The antibody response was analyzed after vaccination with a multiple unpaired T test with Welch correction followed

by a two-stage linear step-up method of Benjamini, Krieger and Yekutieli to correct for multiple comparisons by False Discovery Rate (FDR) (red asterisks, *FDR ≤ 0.01). After challenge, differences between the three groups were assessed using the Kruskal-Wallis test with Dunn's multiple comparison post-hoc test (black asterisks, *P ≤ 0.05; **P ≤ 0.01; ***P ≤ 0.001). (b) Frequency of anti-C. burnetii IgG titers for the Control, Coxevac® and QuilA®-Coxevac® group. Neg = Titers ≤ 40; + = 40 < titers ≤ 100; ++ = 100 < titers ≤ 200; +++ = 200 < titers ≤ 300. (c) Differential IFNγ secretion by PBMCs stimulated with inactivated whole cell C. burnetii. The IFNγ response was analyzed after challenge using mixed-effects models with Geisser-Greenhouse correction (data presented in the result section). 25 IFNγ secretion trends (in black) were visualized via interpolation of cubic splines. = Moment of challenge.

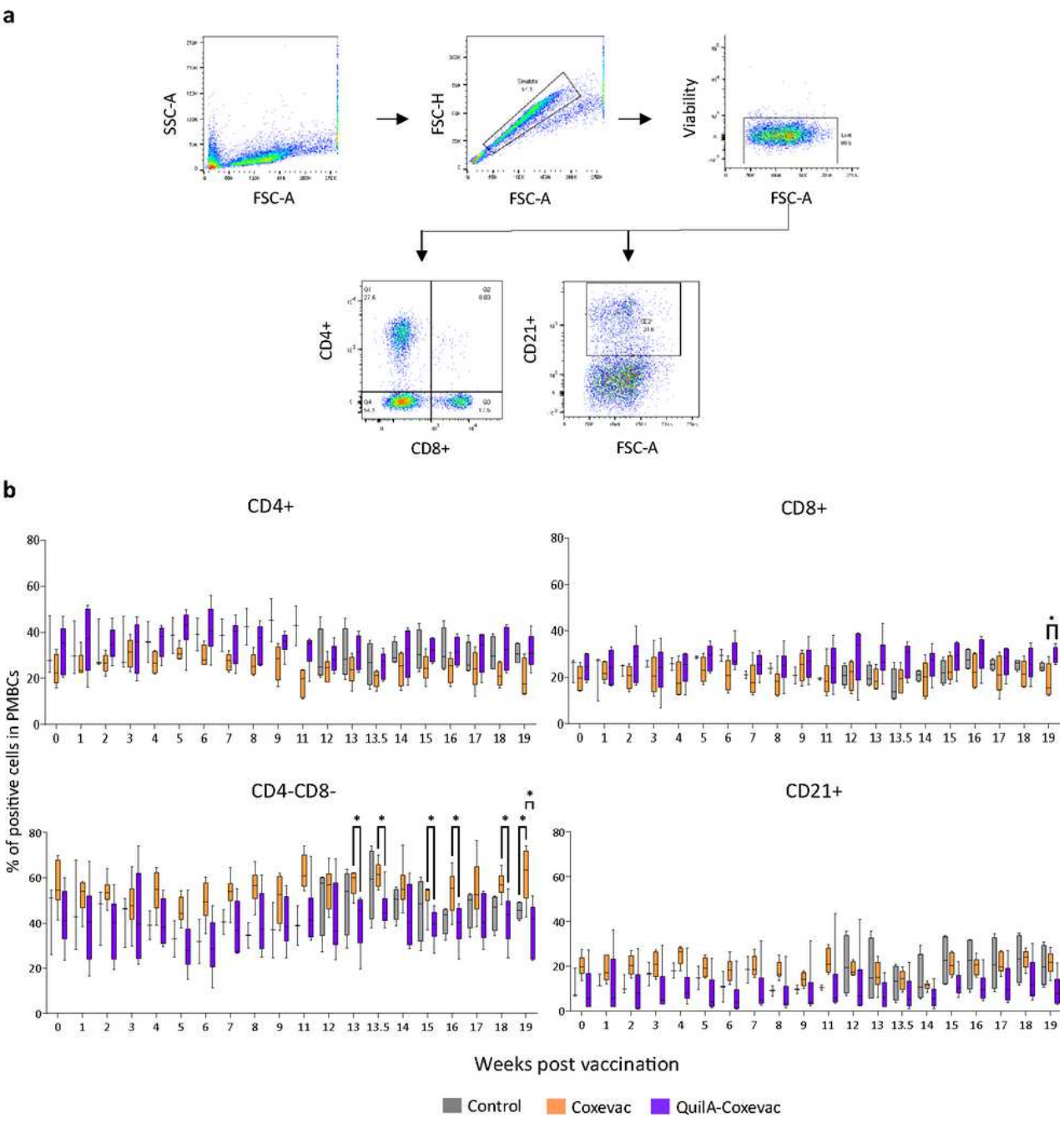

Figure 5

The two Coxevac® formulations activate cell subsets of different nature upon challenge. (a) Gating strategy used in the analysis of T and B lymphocytes in ex-vivo stained PMBCs. Cellular subtypes were identified based on the expression of CD4, CD8 and CD21 cell markers. Plots are from a representative animal. Cell frequencies were calculated as percent of the viable cell population. (b) Kinetics of CD4+, CD8+, CD4-CD8- and CD21 cell frequencies in PBMCs upon vaccination and challenge. Each kinetic was

analyzed using the mixed-effects models, both after vaccination and challenge, with Geisser-Greenhouse correction followed by Tukey's multiple comparison post-hoc test (*P ≤ 0.05). Data are represented as boxplots. w = week after vaccination.

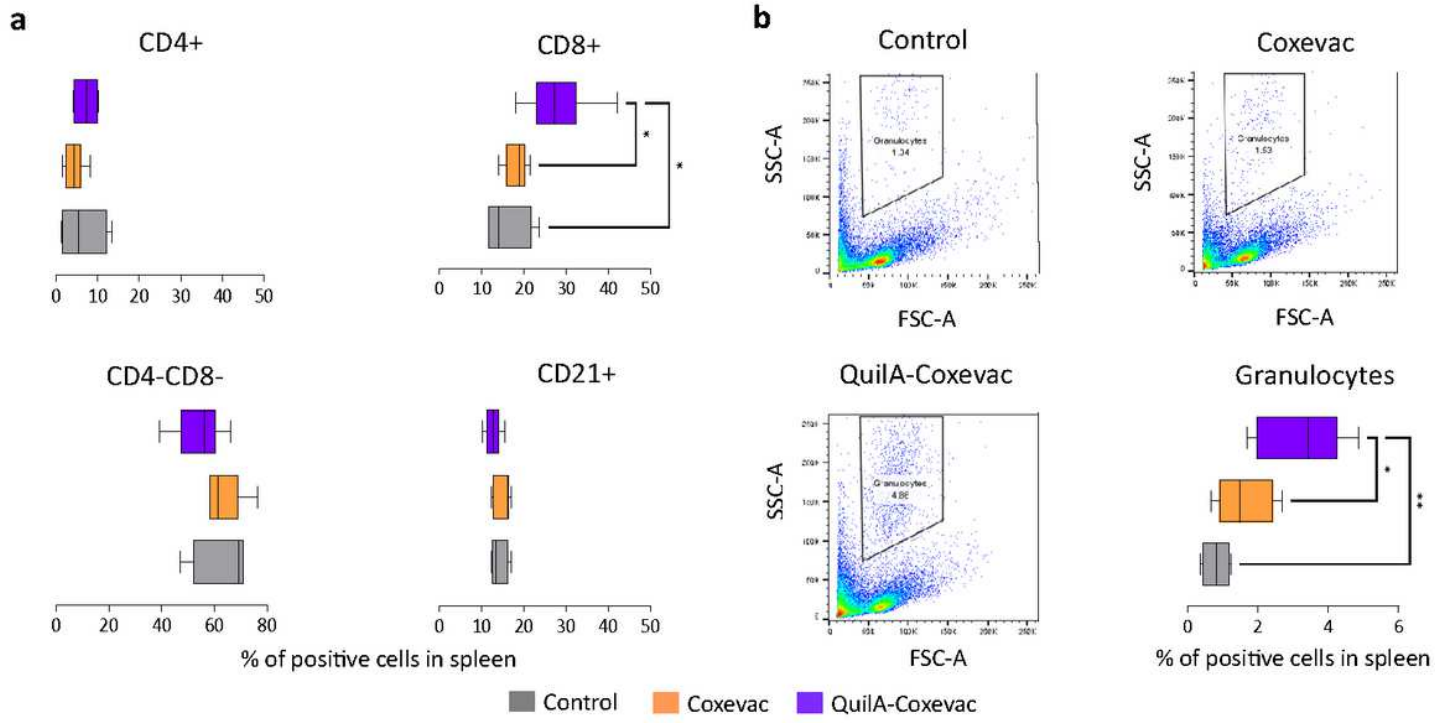

Figure 6

Higher frequencies of CD8+ cells and granulocytes detected in the spleen of the QuilA®- Coxevac® group at sacrifice. (a) Frequencies of CD4+, CD8+, CD4-CD8- and CD21+ cells present in the spleen of Control, Coxevac® and QuilA®-Coxevac® goats. The gating strategy is shown in Figure 5A. (b) Gating strategy used in the analysis of granulocytes observed in goat spleens and quantification of their frequency. The granulocyte population was identified based on size and granularity characteristics. Group comparisons were performed using One-way ANOVA test with Tukey's multiple comparison post-hoc test (*P ≤ 0.05; **P ≤ 0.01; ***P ≤ 0.001) (a-b). Cell frequencies were calculated as percent of the viable cell population and data are represented as boxplots (a-b).

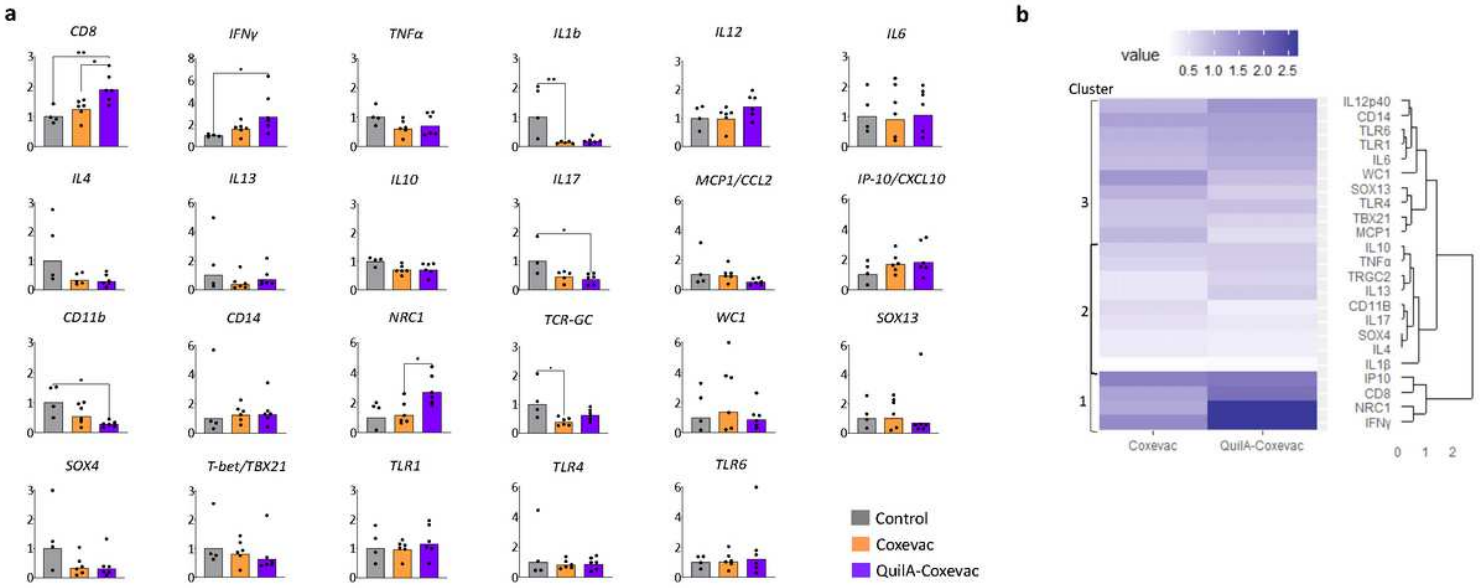

Figure 7

Distinctive transcriptional patterns are induced in spleens of vaccinated and control animals upon challenge. (a) Expression profiles of selected genes (n= 23) in control, Coxevac® and QuilA®- Coxevac® groups at sacrifice. Data are represented as scatter dot plots with a line at the geometric mean. Outliers are identified and removed using the ROUT method (Q=1%). Differences between experimental groups were tested using the One way ANOVA test with Tukey's multiple comparison post-hoc test or the Kruskal-Wallis test with Dunn's multiple comparison post-hoc test depending on the results of the homogeneity of variance and normality of residuals evaluated via the Bartlett's and Shapiro Wilk tests, respectively (*P ≤ 0.05; **P ≤ 0.01; ***P ≤ 0.001). (b) Hierarchical clustering heatmap analysis of data issued from the gene expression profiling in spleen. Each colored cell on the map corresponds to the value of the geometric mean for each group. Values are measured by maximum distance with a Ward.2 clustering algorithm.

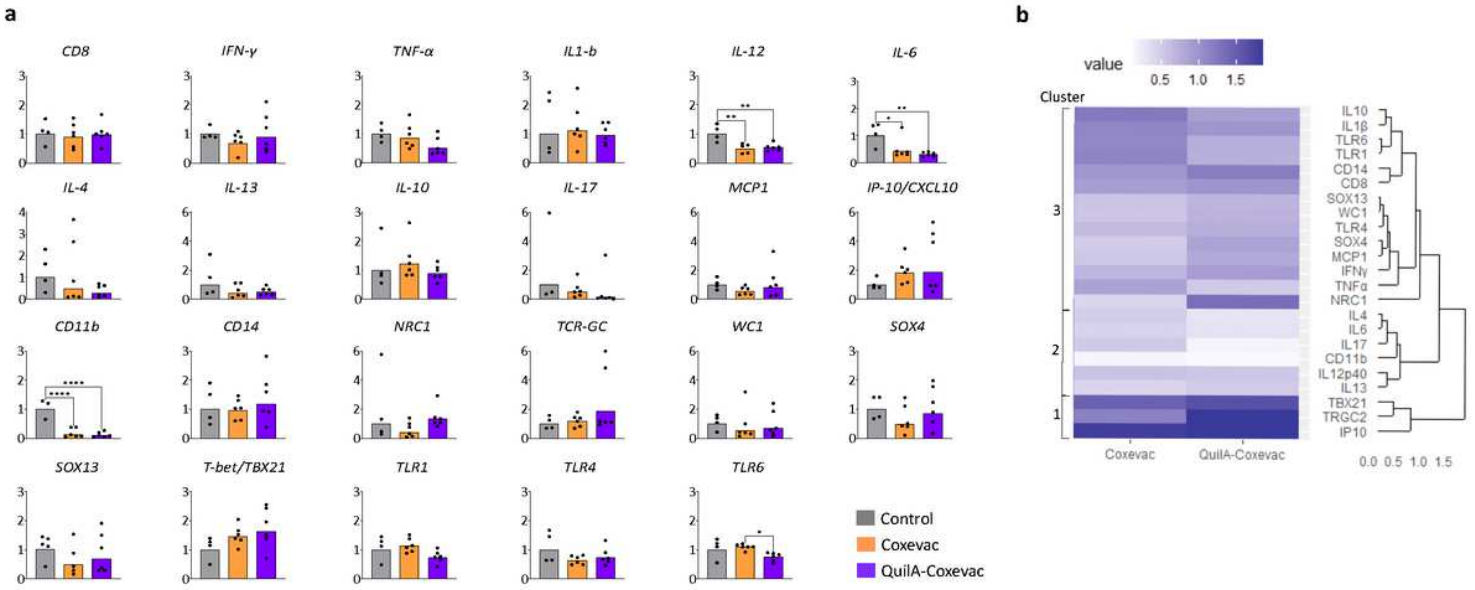

Figure 8

Distinctive transcriptional patterns are induced in bronchial lymph nodes of vaccinated and control animals upon challenge. (a) Expression profiles of selected genes in control, Coxevac® and QuilA®-Coxevac® groups at sacrifice. Data are represented as scatter dot plots with a line at the geometric mean. Outliers are identified and removed using the ROUT method (Q=1%). Differences between experimental groups were tested using the One way ANOVA test with Tukey's multiple comparison post-hoc test or the Kruskal-Wallis test with Dunn's multiple comparison post-hoc test depending on the results of the homogeneity of variance and normality of residuals evaluated via the Bartlett's and Shapiro Wilk tests, respectively (*P ≤ 0.05; **P ≤ 0.01; ***P ≤ 0.001). (b) Hierarchical clustering heatmap analysis of data issued from the gene expression profiling in respiratory lymph nodes. Each colored cell on the map corresponds to the value of the geometric mean for each group. Values are measured by maximum distance with a Ward.2 clustering algorithm.

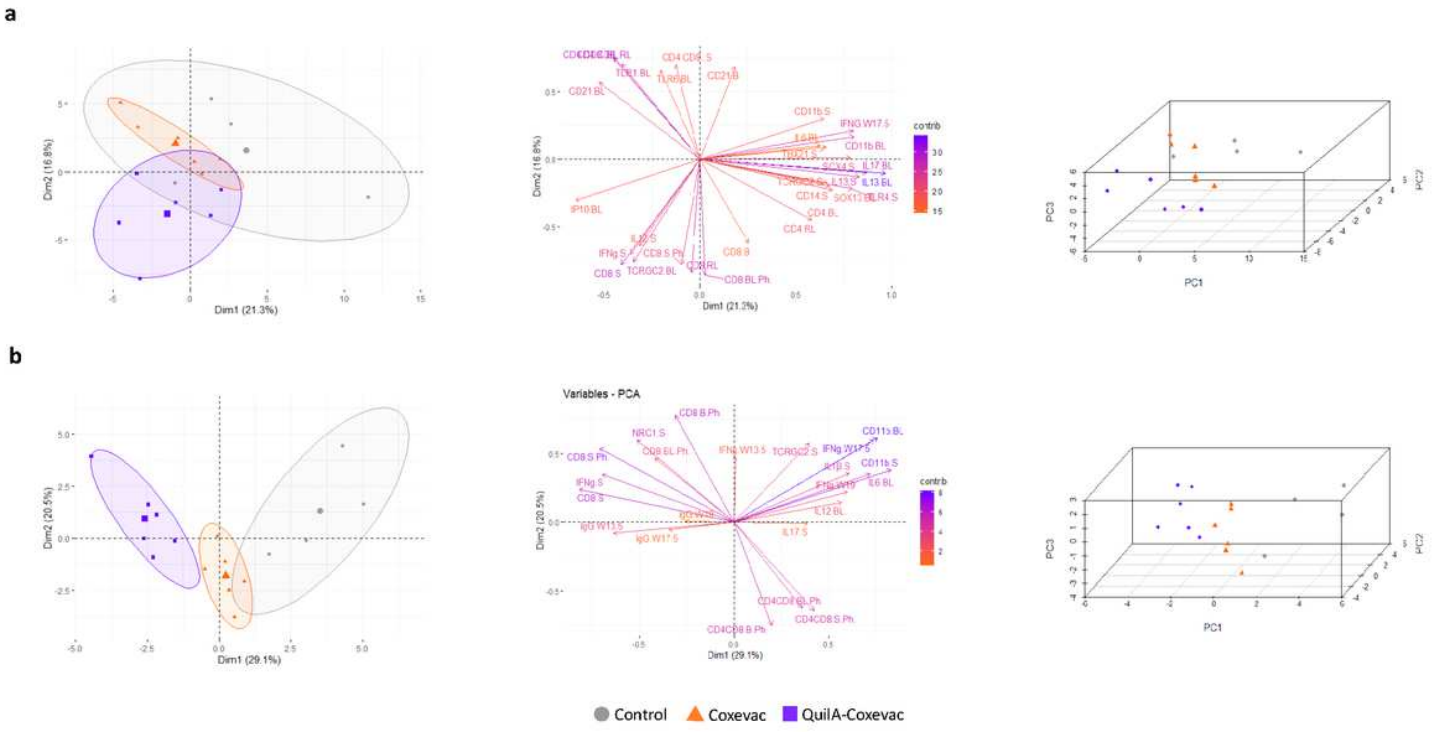

Figure 9

Specific immune responses distinguish Coxevac®, QuilA®-Coxevac® and control goats following C. burnetii challenge. (a) Principal component analysis (PCA) of the complete dataset (n = 68), which included data from serology (weeks 13.5, 17.5 and 19 pv), IFN secretion upon antigen specific stimulated PBMCs (weeks 13.5, 17.5 and 19 pv), organ and blood (week 19 pv) phenotyping and gene expression profiles. (b) PCA of specific selected variables (n= 22) resulting in an accurate 26 separation of the three conditions. From the left, graph 1 is the 2D PCA score plot of the first two components (a-b). Symbols represent animals, the central one corresponds to the mean coordinates of the individuals in the group. Graph 2 is the PCA loading plot showing the distribution of all 22 variables (b) or of variables with a contribution > than 1.5 (n = 31, the loading plot containing all 68 variables is showed in Figure S4) (a). Graph 3 is the 3D PCA score plot of the first three components, realized to increase the proportion of variance illustrated by the analysis (a-b). CD4CD8 = CD4- CD8-, B = blood, S = spleen, BL= bronchial lymph nodes, RL= reproductive lymph nodes, PH = phenotyping, W= week, Contrib = contribution.

Supplementary Files

This is a list of supplementary files associated with this preprint. Click to download.

- Supplementarydata.pdf